FHWA/LA/406	2. Government Accession No.	3. Recipient's Catalog No.
4. Title and Subtitle Development of Models to Estimate the Subgrade and Subbase Layers' Resilient Modulus from In situ Devices Test Results for Construction Control	5. Report Date August 2008 6. Performing Organization Code 02-4B	
7. Author(s) Louay N. Mohammad, Ph.D.; Ananda Herath, Ph.D., P.E; Ravindra Gudishala; Munir D. Nazzal, Ph.D.; Murad Y. Abu-Farsakh, Ph.D., P.E.; and Khalid Alshibli, Ph.D., P.E.	8. Performing Organization Report No. 406	
9. Performing Organization Name and Address Louisiana Transportation Research Center 4101 Gourrier Avenue Baton Rouge, LA 70808	10. Work Unit No. 11. Contract or Grant No. 736-99-1003	
12. Sponsoring Agency Name and Address FHWA Office of Technology Application 400 7th Street, SW Washington, DC 20590 LADOTD P. O. Box 94245 Baton Rouge, LA 70804	13. Type of Report and Period Covered Final Report June 2003-December 2005 14. Sponsoring Agency Code	
15. Supplementary Notes Conducted in Cooperation with the U.S. Department of Transportation, Federal Highway Administration		

16. Abstract

The objective of this study was to develop resilient modulus prediction models for possible application in the quality control/quality assurance (QC/QA) procedures during and after the construction of pavement layers. Field and laboratory testing programs were conducted to achieve this objective. The field testing program included conducting GeoGauge, light falling weight deflectometer, and dynamic cone penetrometer in situ tests. The laboratory program included performing repeated load triaxial resilient modulus tests and physical properties and compaction tests on soil tested in the field. A total of four cohesive soil types and three types of granular materials at different moisture-dry unit weight levels were considered.

Comprehensive statistical analyses were conducted on the field and laboratory test results. Regression models that correlate the resilient modulus to the results of different in situ test devices and soil physical properties were developed. A good agreement was observed between the predicted and measured values of the resilient modulus. The results of this research study demonstrated a promising role of the different in situ tests considered in the QC/QA procedures of the construction of pavement layers.

17. Key Words Resilient modulus, stiffness gauge (GeoGauge), light falling weight deflectometer, dynamic cone penetration, subgrade, cohesive subgrade soils, base, granular materials		18. Distribution Statement Unrestricted. This document is available through the National Technical Information Service, Springfield, VA 21161.	
19. Security Classif. (of this report) N/A	20. Security Classif. (of this page) N/A	21. No. of Pages 82	22. Price N/A

Project Review Committee

Each research project has an advisory committee appointed by the LTRC director. The Project Review Committee (PRC) is responsible for assisting the LTRC administrator or manager in the development of acceptable research problem statements, requests for proposals, review of research proposals, oversight of approved research projects, and implementation of findings.

LTRC appreciates the dedication of the following Project Review Committee members in guiding this research study to fruition.

LTRC Administrator/ Manager

Zhongjie "Doc" Zhang

Members

Bert Wintz	LADOTD
William Oliver	LADOTD
Luanna Cambas	LADOTD
Neal West	LADOTD
Melvin Main	LADOTD
Phil Arena	FHWA
Sam Cooper	LTRC
Kevin Gaspard	LTRC
Gavin Gautreau	LTRC
Michael Boudreaux	LTRC

Directorate Implementation Sponsor

William H. Temple

Chief Engineer, DOTD

Development of Models to Estimate the Subgrade and Subbase Layers' Resilient Modulus from In situ Devices Test Results for Construction Control

by

Louay N. Mohammad, Ph.D.
Professor of Civil and Environmental Engineering
Director, Engineering Materials Characterization Research Facility

Ananda Herath, Ph.D., P.E.
Postdoctoral Researcher

Ravindra Gudishala
Graduate Student

Munir D. Nazzal, Ph.D.
Research Associate

Murad Y. Abu-Farsakh, Ph.D., P.E.
Associate Professor, Research

and

Khalid Alshibli, Ph.D., P.E.
Associate Professor of Civil and Environmental Engineering

LTRC Project No. 02-4B
State Project No. 736-99-1003
FHWA/LA/406

conducted for

Louisiana Department of Transportation and Development
Louisiana Transportation Research Center

August 2008

ABSTRACT

The objective of this study was to develop resilient modulus prediction models for possible application in the quality control/quality assurance (QC/QA) procedures during and after the construction of pavement layers. Field and laboratory testing programs were conducted to achieve this objective. The field testing program included conducting GeoGauge, light falling weight deflectometer, and dynamic cone penetrometer in situ tests. The laboratory program included performing repeated load triaxial resilient modulus tests and physical properties and compaction tests on soil tested in the field. A total of four cohesive soil types and three types of granular materials at different moisture-dry unit weight levels were considered.

Comprehensive statistical analyses were conducted on the field and laboratory test results. Regression models that correlate the resilient modulus to the results of different in situ test devices and soil physical properties were developed. A good agreement was observed between the predicted and measured values of the resilient modulus. The results of this research study demonstrated a promising role of the different in situ tests considered in the QC/QA procedures of the construction of pavement layers.

ACKNOWLEDGMENTS

The U.S. Department of Transportation, Federal Highway Administration (FHWA), Louisiana Department of Transportation and Development (LADOTD), and Louisiana Transportation Research Center (LTRC) financially support this research project.

The assistance of Amar Raghavendra, Paul Brady, Melba Bounds, Aaron Austin, and other LTRC staff in conducting various tests during this study is appreciated.

IMPLEMENTATION STATEMENT

This report presents the development of resilient modulus prediction models for cohesive and granular soils from test results of three in situ devices, namely, dynamic cone penetrometer (DCP), light falling weight deflectometer (LFWD), and GeoGauge. The prediction models developed in this report can be used to estimate the in situ resilient modulus of different pavement layers, which in turn can be utilized to ensure compliance with the resilient modulus values specified in the design procedure. Thus, these models can be implemented in future stiffness based QC/QA procedures during the construction of pavement layers and embankments.

The prediction models developed in this study can also be utilized in conducting forensic analyses of pavement failures by determining the in situ soil resilient modulus in areas where pavement failures have occurred. With this information, an accurate assessment of the soil conditions can be achieved, and an appropriate rehabilitation strategy can be developed. Those models also provide an approach to estimate the resilient modulus values that can be used as input for subgrade and subbase/base materials in the 1993 AASHTO pavement design procedures of new and rehabilitated pavement structures and the new Mechanistic-Empirical Pavement Design Guide.

This study had investigated different in situ devices. The DCP seems to have the most reliable and accurate prediction of in situ resilient modulus (M_r). Based on the results of this study, using this device in future QC/QA procedures of pavement construction is strongly recommended. The LFWD and GeoGauge had comparable results in terms of predicting in situ M_r values. However, more research is needed before recommending those devices to predict the in situ M_r values of pavement layers.

TABLE OF CONTENTS

LIST OF TABLES

LIST OF FIGURES

INTRODUCTION

The current procedure concerning quality control/quality assurance (QC/QA) for the construction of pavement base courses and subgrade is mainly based on performing in-place moisture and in-place density tests *[1]*. The procedure assumes that base courses and subgrade will perform satisfactorily in the field throughout their expected design life as long as an adequate field density is achieved. In general, the field density is measured relative to a maximum dry density under an optimum moisture content determined in laboratory Proctor tests. However, the design parameters of base course and subgrade materials in a pavement design are not based on density values or moisture contents but rather on the material's dynamic engineering strength and/or stiffness values, such as the resilient modulus.

The resilient modulus is defined as the ratio of the maximum cyclic stress to the recoverable elastic strain under repeated loading tests. It is generally referred to as an appropriate measure of stiffness for subgrade and subbase/base materials in a pavement structure. For example, the new Mechanistic-Empirical Pavement Design Procedure Guide (MEPDG) uses the resilient modulus as the primary design input parameter of unbound pavement layers *[2]*.

Since laboratory maximum dry density tests may not provide equivalent or similar strength/stiffness criteria (resilient modulus) as required in the pavement design, a missing link between the design process and the criteria used to evaluate the construction process exists. The missing link makes estimating a stiffness value achieved in the field during the construction process difficult. Therefore, to be able to produce a durable base course and subgrade layer in the field, the procedure used to evaluate construction should have a tool that helps in comparing resilient modulus values achieved during the construction process to the values used in the pavement design.

With the advent of new devices such as GeoGauge and light falling weight deflectometer that assess the QA/QC construction process, estimating stiffness of the pavement layers during the construction process is becoming easier *[3]*. Although the devices can estimate reliable stiffness values of the pavement layers, they are not representative of design stiffness values used in the MEPDG. This is mainly due to (1) stresses applied by the in situ devices not being representative values of traffic loads and (2) in situ devices not being designed for estimating the pavement layers stiffness (resilient modulus). The problem occurring due to the first reason can be solved, to some extent, by correlating the stiffness estimates from in situ devices to the design resilient modulus determined in the laboratory. Thus, the correlations developed in this study will serve the purpose of a tool to estimate the resilient modulus of pavement layers during the construction process.

The aim of this study was to develop resilient modulus prediction models for the cohesive and granular materials from in situ test devices such as dynamic cone penetrometer, GeoGauge, and light falling weight deflectometer and soil physical properties. The results of this research provide a relatively simple, cost-effective, and repeatable approach to estimating the resilient modulus of cohesive and granular soils for use in field verification of the construction resilient modulus that can be compared to that used in the pavement design.

OBJECTIVE

The primary objective of this research was to develop models that predict the resilient modulus of cohesive and granular soils from the test results of various in situ test devices for possible application in QA/QC during construction of pavement structure. The secondary objective was to examine the effects of material type, moisture content, and dry unit weight on the resilient characteristics of investigated cohesive and granular materials.

SCOPE

The scope of this study includes conducting repeated load triaxial tests to determine the resilient modulus of materials similar to the ones used in the recently completed study of "Assessment of In situ Test Technology (AITT) for Construction Control of Base Courses and Embankment" *[4]*.

Laboratory repeated load triaxial resilient modulus tests were conducted on four cohesive soil types and three types of granular materials evaluated at various moisture contents and dry unit weight levels. The four types of cohesive soils included: A-4, A-6, A-7-5, and A-7-6 soils. The three granular materials were crushed limestone, recycled asphalt pavements (RAP), and sand. The AITT study conducted tests in both the laboratory and the field on the above materials using three in situ devices (DCP, GeoGauge, and LFWD). The AITT study also included conducting material property tests, such as gradation characteristics, moisture content, unit weight, standard Proctor, and modified Proctor. It is noted that DCP test results from a recently completed study at the LTRC were also incorporated in the DCP model development *[5]*.

METHODOLOGY

Background

Resilient Modulus (M_r)

The resilient modulus is a fundamental engineering material property that describes the non-linear stress-strain behavior of pavement materials under repeated loading. It is defined as the ratio of the maximum cyclic stress (σ_{cyc}) to the recoverable resilient (elastic) strain (ε_r) in a repeated dynamic loading, as shown in the following equation:

$$M_r = \frac{\sigma_{cyc}}{\varepsilon_r} \tag{1}$$

The M_r is typically determined in the laboratory through conducting repeated load triaxial (RTL) tests on representative material samples. Several empirical correlations have been developed to predict the results of the resilient modulus test. The AASHTO recommends equations (2) and (3) for granular and cohesive soil materials, respectively.

$$M_r = k_1 \theta^{k_2} \tag{2}$$

$$M_r = k_3 \sigma_d^{\ k_4} \tag{3}$$

where,

M_r – resilient modulus;

σ_d – deviator stress = σ_1 - σ_3, σ_1- major principal stress;

σ_2 – intermediate principal stresses, σ_3 -minor principal stress;

θ – bulk stress =σ_1+ σ_2+σ_3; and

k_1 , k_2 , k_3,and k_4 – material constants.

It is noted that the model presented in equation (2), also known as the bulk stress model, does not show the individual effects of the deviator and confining stresses. The model presented in equation (3), also known as the deviator stress model, does not show the significance of the confining stress on cohesive soil.

Mohammad et al. proposed an octahedral stress model to overcome some of the limitations discussed above *[6]*. The model takes into account the effects of shear and influence of the stress state. The model can be used for both cohesive and granular soils. The model considers the octahedral shear and normal stresses. The octahedral model is given as follows:

$$\frac{M_r}{\sigma_{atm}} = k_1 \left(\frac{\sigma_{oct}}{\sigma_{atm}} \right)^{k_2} \left(\frac{\tau_{oct}}{\sigma_{atm}} \right)^{k_3} \tag{4}$$

where,
M_r is the resilient modulus;
k_1, k_2, and k_3 are material constants;
σ_{oct} is the octahedral normal stress;
τ_{oct} is the octahedral shear stress; and
σ_{atm} is the atmospheric pressure = 14.7 psi (101.35 kPa).

The AASHTO 1993 and the MEPDG have adopted the use of resilient modulus as a material property in characterizing pavements for their structural analysis and design. It is noted that the MEPDG *[2]* provides the users with three levels to input the M_r value. At input Level I, the M_r value is determined using the laboratory tests based on the generalized model shown in equation (5):

$$\frac{M_r}{P_a} = k_1 \left(\frac{\theta}{P_a} \right)^{k_2} \left(\frac{\tau_{oct}}{P_a} + 1 \right)^{k_3} \tag{5}$$

where,
M_r = resilient modulus,
θ = bulk stress = $\sigma_1+\sigma_2+\sigma_3$,
σ_1 = major principal stress,
σ_2 = intermediate principal stress,
σ_3 = minor principal stress/confining pressure,
$\tau_{oct} = \frac{1}{3}\sqrt{(\sigma_1-\sigma_2)^2+(\sigma_1-\sigma_3)^2+(\sigma_2-\sigma_3)^2}$,
P_a = normalizing stress (atmospheric pressure) = 14.7 psi (101.35 kPa), and
k_1, k_2, k_3 = material constants.

Different approaches can be used to estimate the M_r. These include the use of empirical correlations with the soils' physical and strength properties. During the last three decades, various empirical correlations have been proposed and used to predict M_r. Van Til et al. *[7]* related M_r of subgrade soils to the soil support value (SSV) employed in the earlier AASHTO design equation. They also made a correlation chart in which the values of M_r can be determined by the internal friction of R-value, CBR, and the Texas triaxial classification value. Many other correlations between M_r, CBR, R-value, and soil support values were also developed *[3]*. The Louisiana Department of Transportation and Development (LADOTD) has historically estimated the M_r of subgrade soils based on the soil support value (SSV) using the following equation:

$$M_r = 1500 + 450\left(\left(\frac{53}{5}\right)(SSV - 2)\right) - 2.5\left(\left(\frac{53}{5}\right)(SSV - 2)\right)^2 \tag{6}$$

where,
M_r = resilient modulus (psi), and
SSV = soil support value.

The SSV is obtained from a database based on the parish system in Louisiana. Currently, the LADOTD uses a typical M_r value for each parish instead of obtaining subgrade M_r values for each project. This can lead to inaccuracies in pavement design, as the subgrade M_r can vary from site to site within the parish as well as seasonally.

Another alternative for estimating the M_r is the use of in situ test devices. Different devices have been proposed and used during the last decades. The following sections provide a brief background of the in situ devices investigated in this study.

In situ and Nondestructive Test Methods

The field tests conducted in this research included the light falling weight deflectometer, GeoGauge, and dynamic cone penetration. The following section provides a brief description for each test.

Stiffness Gauge (GeoGauge) Test Device

GeoGauge is a portable, quick, economical, and reliable in situ device that is used for estimating in situ stiffness of subgrade and subbase/base materials. The GeoGauge evolved from the defense technology and is manufactured by Humboldt Manufacturing Co. *[3]*. The GeoGauge (Figure 1) weighs about 10 kg and is capable of measuring small deflections under small loads. It consists of a mechanical shaker attached to the foot with an onboard battery, a seating foot, and special sensors. The ring shaped foot of the GeoGauge rests on the subgrade and subbase/base materials to be tested. The shaker generates vibrations from 100 to 200 Hz in 4 Hz increments that make 25 different frequencies on the seating foot. The GeoGauge measures the force and deflection-time history of the foot. Sawangsuriya et al. *[8]* measured the dynamic loading under the GeoGauge and reported the single amplitude of the dynamic force of 9 N at frequencies ranging from 100 to 200 Hz.

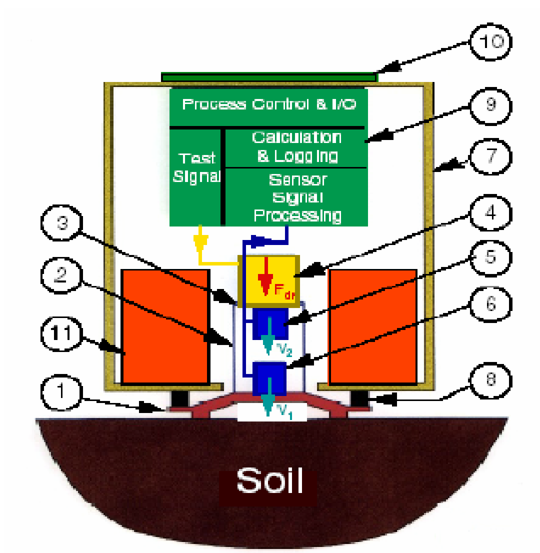

1. Rigid foot with annular ring
2. Rigid cylindrical sleeve
3 Clamped flexible plate
4. Electro mechanical shaker
5. Upper velocity sensor
6. Lower velocity sensor
7. External case
8. Vibration isolation mounts
9. Electronics
10. Control & supply
11. Power supply

Figure 1
Stiffness gauge

The modulus of material can be derived from the GeoGauge measured stiffness using the theory of elasticity, Poisson's ratio, and geometry of the device. Egorov *[9]* provided the solution for a rigid annular ring on a linear elastic, homogeneous, isotropic half space. The relationship between the modulus (E_{geo}) and stiffness (K) can be expressed as:

$$E_{geo} = \frac{K(1-\nu^2)\omega(n)}{r} \tag{7}$$

where,

E_{geo} = modulus of elasticity from the GeoGauge™ test (MPa),

K = material stiffness from the GeoGauge™ (MN/m),

ν = Poisson's ratio,

$\omega(n)$ = 0.565 for the GeoGauge™ geometry, and

r = radius of the GeoGauge™ ring (0.05715 m).

Light Falling Weight Deflectometer (LFWD) Test Device

The LFWD was originally developed in Germany *[10]*. The LFWD test has widely been used in geotechnical investigations and road construction for determining the soil bearing capacity and compaction. As a simple, easy handling, portable, economical, timesaving, and user-friendly in situ device, the LFWD has been used in pavement engineering as a tool in estimating the pavement deflection under an impulse load.

The LFWD device (Figure 2), Prima 100, from the Carl Bro Pavement Consultants in Denmark, was used in this research *[11]*. The Prima 100 consists of a center geophone, loading plate (200 mm in diameter), load cell, and 10 kg hammer. The geophone measures the deflection caused by freely dropping the hammer from a height of 850 mm onto the loading plate. The falling weight produces a load pulse of 1-15 kN in 15-20 milliseconds. Both the deflection and force are recorded to compute the stiffness of the pavement structure by performing Boussinesq static analysis. The following equation is used to estimate the LFWD dynamic modulus (E_{lfwd}):

$$E_{lfwd} = \frac{K(1-\nu^2)}{\delta_c}\mathrm{Pr} \tag{8}$$

where,

E_{lfwd} = *LFWD* dynamic modulus (psi);

K = π/2 or 2 for rigid and flexible plates, respectively;

δ_c = center deflection (in.);

ν = Poisson's ratio;

r = radius of loading plate (in.); and

P = applied stress (psi).

Figure 2
LFWD device

Dynamic Cone Penetrometer (DCP) Test Device

DCP is a portable instrument that consists of an 8 kg sliding hammer, anvil, pushing rod (diameter 16 mm), and steel cone tip, as shown in Figure 3a. The cone tip angle is 60 degrees, and its diameter is 20 mm. The diameter of the pushing rod is less than that of the cone base. This design assists in reducing the frictional forces along the wall of the cone penetrometer. The DCP test consists of pushing a conical tip attached to the bottom of the pushing rod into the soil layer and measuring the resistance to penetration.

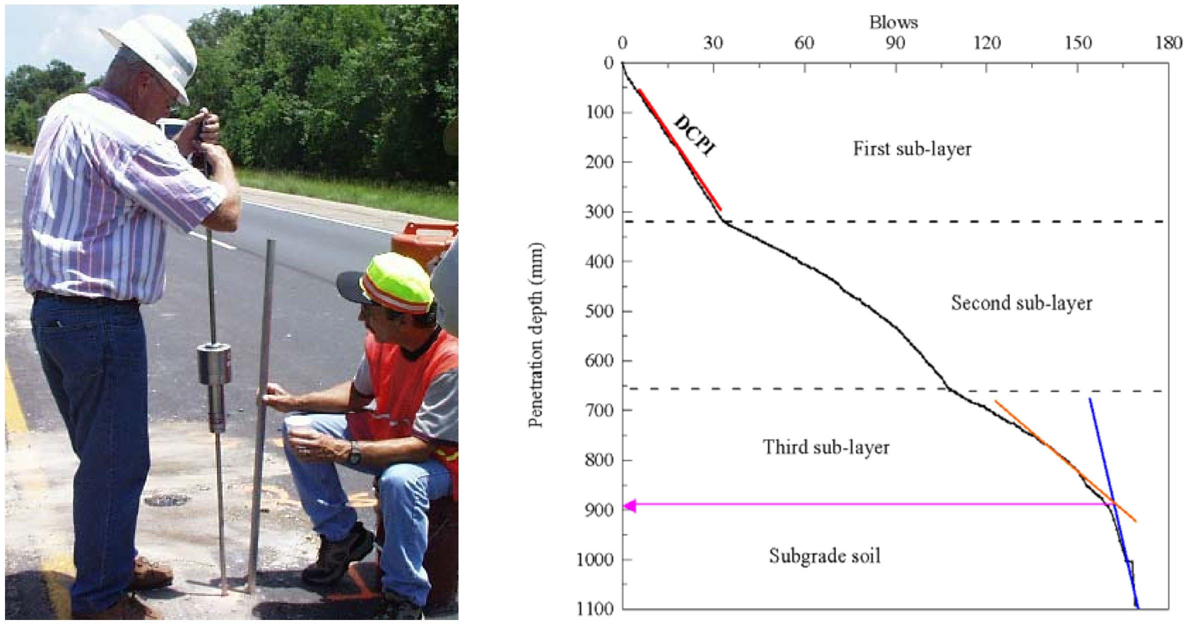

(a) **(b)**

Figure 3
Dynamic cone penetration test
(a) The DCP test (b) A typical DCP profile

Table 1
M_r-DCP correlations reported in literature

Study	Correlation	Soil type	Comment
Hasan *[12]*	$M_r = 7013.065 - 2040.783\ln(DCPI)$	Cohesive	M_r in psi, DCPI in in/blow
George et al. *[13]*	$M_r = a_o\left(DCPI\right)^{a1}\left(\gamma_{dr}{}^{a2} + \left(LL/w_c\right)^{a3}\right)$	Cohesive	Mr in psi, DCPI in in/blow; W_c is moisture content; LL is liquid limit ; c_u is coefficient of uniformity; $w_{cr} = \frac{\text{field moisture}}{\text{optimum moisture}}$; and $\gamma_{dr} = \frac{\text{field } \gamma_d}{\text{maximum } \gamma_d}$ a_o, a_1, a_2 and a_3 model coefficients.
	$M_r = a_o(DCPI/\log c_u)^{a1}(w_{cr}{}^{a2} + \gamma_{dr}{}^{a3})$	Granular	

During the past decades, the DCP measurement has been correlated to many engineering properties such as the CBR, shear strength, and elastic modulus. In addition, different models were developed to predict the laboratory measured M_r using DCP test results. A summary of the models is presented in Table 1. The MEPDG software also used the DCP results to estimate the M_r values of different pavement layers by first computing the California Bearing Ratio (CBR) using the CBR-DCP relation proposed by Webster, equation (9), and then predicting M_r based on the M_r-CBR relation suggested by Powell et al., equation (10) *[14], [15]*. However, since the CBR is estimated using a static test, these types of correlations do not take into account the dynamic behavior of pavements under moving vehicles.

$$CBR = \frac{292}{DCPI^{1.12}} \tag{9}$$

$$M_r = 17.58\,(CBR)^{0.64} \tag{10}$$

where,
M_r = resilient modulus in MPa, and
DCPI = penetration Index, mm/blow.

Field and Laboratory Testing Program

Field and laboratory testing programs were performed on cohesive and granular materials. A detailed description of field and laboratory testing can be found elsewhere *[4], [5]*. The results from all three in situ test devices, namely GeoGauge, DCP, and LFWD, were collected from the AITT report *[4]*. Tables 2 and 3 show the test factorial of the AITT study. The following is a brief description of the method of preparation of test layers and testing procedures used in both the laboratory and the field to conduct the in situ tests. However, for a detailed description of test procedures, readers are advised to refer to the original AITT report *[4]*.

Field Testing

The field testing program included testing different types of cohesive and granular soils at several sections. In each test section, five LFWD and Geogauge tests and two DCP tests were conducted. The dry unit weight and moisture content were also measured using the nuclear density gauge device. Samples for each tested material were secured for the laboratory testing program. Further details of the field tests can be found elsewhere *[4, 5]*.

Table 2
Test factorial of cohesive subgrade soils *[4]*

Type of Material	Soil ID	Location	w (%)	γ_d (pcf)
Clay	Clay-1	Lab	11.0	110.9
	Clay-2	Lab	12.5	117.8
	Clay-3	Lab	14.6	104.6
	Clay-4	Lab	13.9	117.2
	Clay-5	Lab	8.4	95.8
	Clay-6	Lab	9.4	106.5
	Clay-7	Lab	13.3	109.6
Clayey Silt	Clayey Silt-1	Lab	19.0	101.4
	Clayey Silt-2	Lab	15.4	100.2
	Clayey Silt-3	Lab	20.1	100.8
	Clayey Silt(ALF)	Field	18.5	104.0
Clay	LA-182	Field	21.2	100.2
	US-61	Field	15.6	100.8

Legend: w – Moisture content, γ_d – Dry unit weight, Lab – Laboratory

Table 3
Test factorial granular base materials *[4]*

Type of Material	Soil ID	Location	w (%)	γ_d (pcf)
Crushed Limestone	CL1-1	Field	4.8	117.8
	CL1-2	Field	5.2	120.3
	CL1-3	Field	5.6	132.9
	CL1-4	Lab	6.1	121.6
	CL2	Lab	3.2	123.5
Sand	Sand-1	Lab	2.0	111.5
	Sand-2	Lab	2.5	102.7
	Sand-3	Lab	2.2	101.4
	Sand-4	Field	3.3	101.4
	Sand-5	Field	2.9	108.4
	Sand-6	Field	2.7	109.0
Recycled Asphalt Pavement	Rap-1	Field	11.9	99.6
	Rap-2	Field	11.4	106.5
	Rap-3	Field	11.6	113.4
	Rap-4	Lab	13.3	107.7

Legend: w – Moisture content, γ_d – Dry unit weight, Lab – Laboratory

Laboratory Testing

Laboratory tests consisted of the determination of resilient modulus and properties of investigated materials. Laboratory repeated load triaxial M_r tests were performed on samples obtained close to the LFWD, GeoGauge, and DCP test locations. For cohesive soils, cylindrical specimens of 71.1 mm (diameter) by 142.2 mm (height) were compacted in five layers using an impact compactor for the laboratory repeated load triaxial M_r tests. The laboratory resilient modulus test was conducted according to the AASHTO procedure T 294-94 *[16]*, while, for granular materials, cylindrical specimens of 152.4 mm (in diameter) x 304.8 mm (in height) were compacted for laboratory resilient modulus tests. The samples were compacted in six (50 mm) layers. An electric vibratory hammer was used for compaction. The same moisture content and dry unit weight levels used in the corresponding LFWD, GeoGauge, and DCP tests were selected in the laboratory soil sample compaction for the M_r tests. Three sample replicates were tested in the resilient modulus test. Material property tests were also performed (Table 4). Tables 5 and 6 present a summary of properties of the cohesive and granular materials investigated in this study. It is noted that two different gradations of crushed limestone were included.

Table 4
Material classification test procedures

Test	LADOTD	AASHTO / ASTM
Sample preparation	TR 411M/411-95	T87-86
Hydrometer	TR 407-89	T88-00
Atterberg limits	TR 428-67	T89-02, T90-00
Moisture/Density curves	TR 418-93	T-99-01, T180-01
Sieve analysis	TR 113-75	T88-00, T27-99, ASTM C136
Organic content	TR 413-71	T194-97
Moisture content	TR 403-92	T 265

Table 5
Physical properties of cohesive subgrade materials

Type of Soil	Clayey Silt	Clay	Clay	Clay
Location	Lab	Lab	Field	Field
Soil ID	Clayey Silt	Clay	US-61	LA-182
LL	27	31	31	22
PL	21	16	18	18
PI	6	15	13	4
Sand(%)	9	35	31	59
Silt(%)	72	37	41	28
Clay(%)	19	28	28	14
Maximum dry density(KN/m^3) γ_d	17.5	18.5	16.5	17.5
Optimum moisture content (%) w_{opt}	18.6	13.1	16.4	17.1
AASHTO classification	A-4	A-6	A-6	A-4
USCS classification	CL-ML	CL	CL-ML	CL-LM

Table 6
Gradation analysis of granular base materials

Sieve Size		Crushed Limestone		Sand	Recycled Asphalt Pavement
mm	inch	Gradation 1	Gradation 2		
62.50	2 1/2	100	100	100	100
50.00	2	100	100	100	96.5
37.50	1 1/2	100	100	100	95.9
25.00	1 1/4	98.4	98.8	100	94.3
19.00	1	94.3	96.6	100	92.7
19.05	3/4	83.8	87.9	100	89.1
15.88	5/8	78.4	82.2	100	85.8
12.70	1/2	72.2	75.9	100	80.8
9.53	3/8	65.6	67.5	100	71.4
4.75	No.4	52.7	50.4	99.0	51.8
2.36	No.8	33.7	36.3	95.8	36.5
1.18	No.16	30.6	33.4	89.4	33.9
0.85	No.20	24.5	26.3	-	27.1
0.60	No.30	20.3	19.6	68.5	19.3
0.42	No.40	18.5	17.1	-	13.9
0.30	No.50	17.1	15.0	10.5	9.7
0.18	No.80	16.4	13.4	-	4.9
0.15	No.100	15.3	12.5	0.6	3.1
0.075	No.200	12.9	10.6	0.2	0.5
AASHTO (Classification)		A-1-a	A-1-a	A-3	A-1-a
USCS (Classification)		GC	GW	SP	GP
Optimum water content (%)		5.9	3.2	4.2	8.6
Maximum dry density (kN/m^3)		22.0	19.8	17.1	18.6

DISCUSSION OF RESULTS

The main focus of this study was to develop models to predict the resilient modulus of cohesive and granular materials using the results of the LFWD, GeoGauge, and DCP test data, material properties, moisture content, and dry unit weight.

Prior to the development of the models, a field representative M_r value was defined, and test results (tables 7 through 11) were analyzed to evaluate the effect of stress levels, moisture content, dry unit-weight, and material properties on the resilient modulus, LFWD, GeoGauge, and DCP test results of cohesive and granular materials. The DCP test results from other studies were also incorporated into the model development *[4]*, *[5]*. Finally, prediction models of the M_r were developed.

A Field Representative Resilient Modulus Value

Based on the stress estimations of the subgrade resulting from the traffic loading, a field representative cyclic stress of approximately 41.3 kPa (6 psi) and a confining stress of approximately 14 kPa (2 psi) were selected to interpolate the corresponding M_r value from the repeated load triaxial test results *[17]*. For granular base materials, a cyclic stress of approximately 103.35 kPa (15 psi) and a confining pressure of approximately 34.45 kPa (5 psi) were selected *[17]*. The interpolated M_r was considered as the measured M_r from the laboratory repeated load triaxial test.

Development of M_r Prediction Models for Cohesive Soils from DCP Test Results

Tables 7 and 8 present the combined DCP and M_r results that were used in developing regression models that predict the laboratory measured M_r from the DCP test results. It is noted that Table 8 includes DCP test results from a recently completed project at LTRC *[5]*. The ranges of variables used in the regression analysis are presented in Table 9. In order to determine the independent variables that should be included in the multiple regression analysis, possible linear correlations between the dependent variable M_r and DCPI, Log (DCPI), 1/DCPI, dry unit weight (γ_d), water content (w), and γ_d/w were first considered. Figures 4 through 9 present the scatter plots between the dependent variable and independent variables. It is noted that as the DCPI increases, the M_r decreases. This implies that soil stiffness decreases as the DCPI increases. Therefore, a good linear correlation between the inverse of DCPI and M_r may exist. Figures 7 and 8 demonstrate that the laboratory measured M_r increases with the increase in the dry unit weight and the decrease in the water content. Finally, Figure 9 shows the variation of M_r with the γ_d/w. It is noted that as the γ_d/w increases, M_r increases.

Table 7
Resilient modulus and DCP test results of cohesive subgrade soils

Type of Material	Soil ID	Location	M_r (ksi)	CV (%)	Std. (ksi)	DCPI (mm/blow)
Clay	Clay-1	Lab	10.4	12	1.2	17
	Clay-2	Lab	12.0	7	0.8	16.7
	Clay-3	Lab	8.3	9	0.7	23
	Clay-4	Lab	12.1	10	1.1	13
	Clay-5	Lab	9.7	4	0.3	18.4
	Clay-6	Lab	10.1	11	1.0	15
	Clay-7	Lab	10.2	2	0.2	22.5
Clayey Silt	Clayey Silt-1	Lab	7.0	1	0.0	26.1
	Clayey Silt-2	Lab	9.7	1	0.1	18.8
	Clayey Silt-3	Lab	7.2	8	0.4	27
	Clayey Silt(ALF)	Field	6.2	8	0.5	29
Clay	LA-182	Field	5.6	11	0.6	36.0
	US-61	Field	9.0	16	1.4	10.2

Legend: CV – Coefficient of variation, Std. – Standard deviation, and DCPI – DCP penetration index, M_r – Measured Resilient modulus, Lab – Laboratory

Table 8
DCP and M_r test results *[5]*

Project	Site/Soil ID	ID	M_r (ksi)	DCPI (mm/blow)	Project	Site/Soil ID	ID	M_r (ksi)	DCPI (mm/blow)
LA333	A	2	6.3	18.8	LA347	A	2	9.0	13.7
		5	4.5	21.5			5	12.7	9.9
		8	5.8	20.7			8	9.1	12.5
	B	2	5.7	21.0		B	2	12.0	11.0
		5	3.8	24.4			5	10.5	12.0
		8	2.7	21.6			8	10.7	11.6
	C	2	3.9	20.0		C	2	8.1	14.0
		5	3.3	24.4			5	7.6	17.8
		8	6.0	18.9			8	8.4	13.9
US171	A	2	2.2	34.4	LA991	A	2	4.4	27.2
		5	3.4	30.5			5	4.3	27.9
		8	3.5	30.8			8	4.4	24.8
	B	2	3.5	30.0		B	2	4.3	25.9
		5	7.2	17.2			5	4.5	26.0
		8	4.5	26.8			8	4.5	26.0
	C	2	13.3	9.6		C	2	3.8	22.0
		5	10.2	12.1			5	3.7	26.9
		8	9.3	12.9			8	3.5	23.0
LA22	A	2	5.8	20.0	LA28	A	2	4.8	35.3
		5	5.7	19.0			5	4.0	41.0
		8	5.6	23.0			8	4.9	37.0
	B	2	5.7	18.0		B	2	12.6	9.0
		5	7.8	14.9			5	10.3	12.0
		8	8.6	13.0			8	10.5	13.0
	C	2	5.6	21.0		C	NA	NA	NA
		5	5.9	20.0			NA	NA	NA
		8	5.6	23.0			NA	NA	NA
LA344	A	2	4.4	21.0	LA182	A	2	3.8	34.1
		5	4.2	24.5			5	3.6	38.0
		8	4.3	24.5			8	4.6	28.9
	B	2	4.5	18.9		B	2	3.8	30.1
		5	4.6	21.4			5	5.1	23.4
		8	4.6	31.3			8	4.1	36.8
	C	2	5.7	18.2		C	2	2.8	30.0
		5	5.5	19.3			5	3.4	35.1
		8	6.0	18.6			8	2.7	53.3
LA652	A	2	1.9	85.1	Legend: DCPI – DCP penetration index, M_r – Measured Resilient modulus, NA – Not applicable				
		5	1.1	65.2					
		8	2.6	47.0					
	B	2	4.7	40.0					
		5	2.7	27.2					
		8	5.6	28.1					
	C	2	0.9	44.2					
		5	1.8	42.3					
		8	2.2	46.0					

Table 9
Ranges of variables of cohesive materials used in DCP model development

Property	Range for A-4 soils	Range for A-6 soils	Range for A-7-5 soils	Range for A-7-6 soils
No. of samples	6	26	45	15
M_r (ksi)	5-10	4-14	1-14	3-9
DCPI (mm/blow)	19-36	10-28	9-65	13-41
PI (%)	4-6	12-23	27-61	15-43
γ_d (pcf)	100-104	96-118	57-113	84-108
w (%)	15-24	8-27	21-60	18-35
LL (%)	22-28	27-40	46-98	41-62
Sand (%)	7-58	11-35	4-28	3-32
Silt (%)	28-72	37-72	9-62	23-58
Clay (%)	14-23	8-32	27-86	32-53
Passing sieve #200 (%)	42-93	65-89	72-96	68-97

Legend: M_r – Resilient modulus, DCPI – DCP penetration index, PI – Plasticity index, w – Water content, LL – Liquid limit, Silt – Percentage of silt, Clay – Percentage of clay, γ_d – Dry unit weight

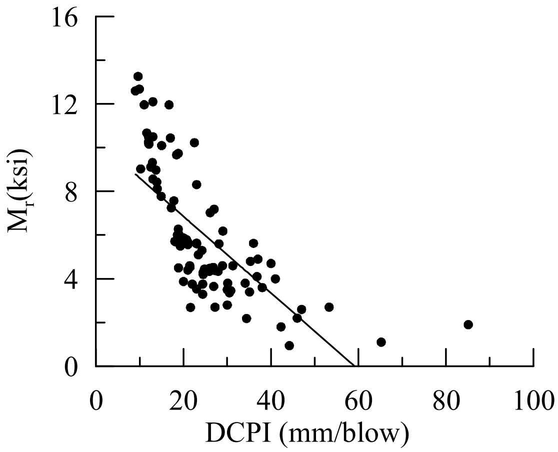

Figure 4
Variation of M_r with DCPI

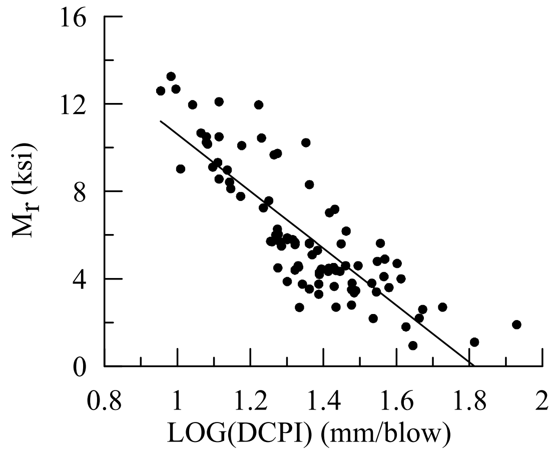

Figure 5
Variation of M_r with log (DCPI)

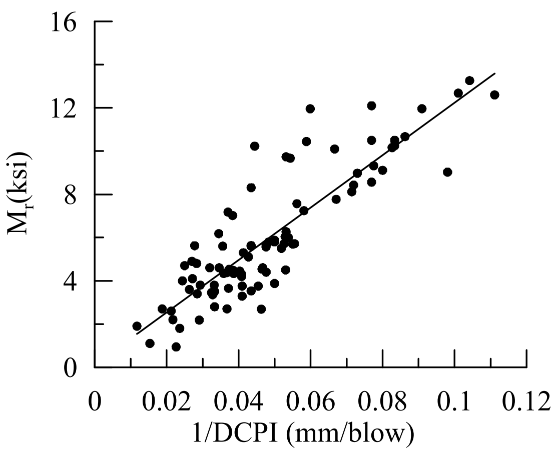

Figure 6
Variation of M_r with 1/DCPI

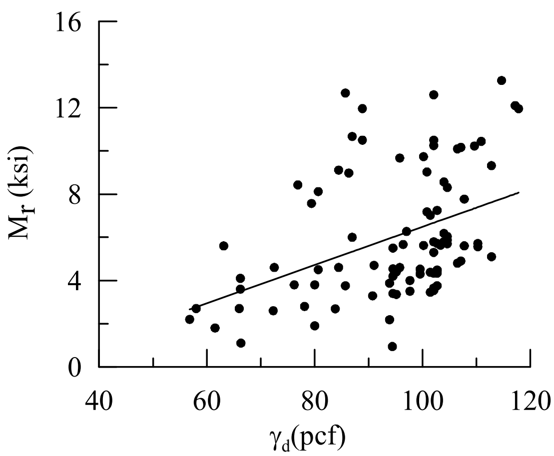

Figure 7
Variation of M_r with γ_d

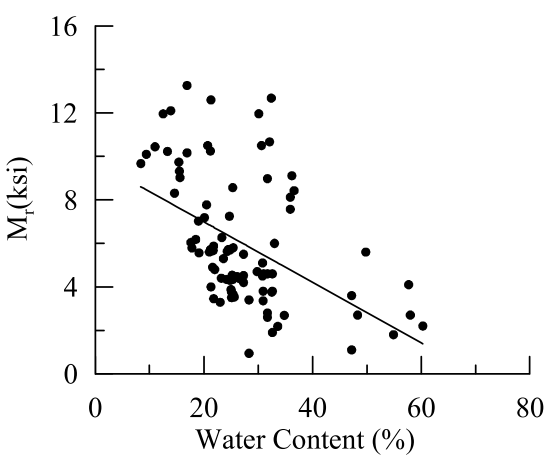

Figure 8
Variation of M_r with water content

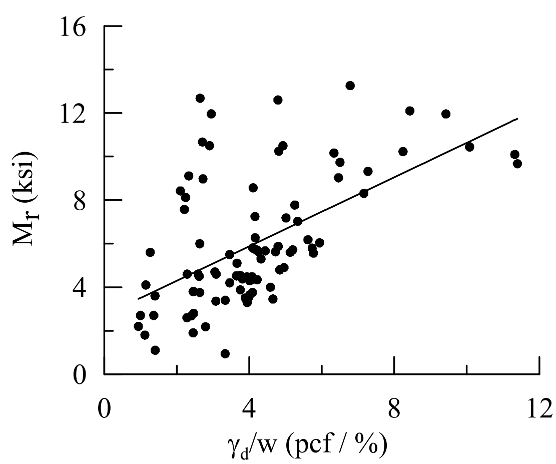

Figure 9
Variation of M_r with γ_d/w

Table 10
A correlation matrix for the DCP test results (p-value)

	γ_d	w	M_r	DCPI	γ_d /w	#200	%Silt	%Clay	LL	PI	Log (DCPI)	1/DCPI
γ_d	-	<0.001	<0.001	<0.001	<0.001	<0.001	0.32	<0.001	<0.001	<0.001	<0.001	<0.001
w	<0.001	-	<0.001	<0.001	<0.001	<0.001	0.28	<0.001	<0.001	<0.001	<0.001	<0.001
M_r	<0.001	<0.001	-	<0.001	<0.001	0.24	0.44	0.009	0.09	0.21	<0.001	<0.001
DCPI	<0.001	<0.001	<0.001	-	<0.001	0.15	0.98	0.40	0.05	0.004	<0.001	<0.001
γ_d /w	<0.001	<0.001	<0.001	<0.001	-	<0.001	0.81	<0.001	<0.001	<0.001	<0.001	<0.001
-# 200	<0.001	<0.001	0.24	0.15	<0.001	-	0.006	<0.001	<0.001	<0.001	0.19	0.22
%Silt	0.32	0.28	0.44	0.98	0.81	0.006	-	<0.001	<0.001	<0.001	0.03	0.38
%Clay	<0.001	<0.001	0.009	0.40	<0.001	<0.001	<0.001	-	<0.001	<0.001	0.003	0.10
LL	<0.001	<0.001	0.09	0.05	<0.001	<0.001	<0.001	<0.001	-	<0.001	0.03	0.042
PI	<0.001	<0.001	0.21	0.004	<0.001	<0.001	<0.001	<0.001	<0.001	-	0.10	0.68
Log (DCPI)	<0.001	<0.001	<0.001	<0.001	<0.001	0.19	0.03	0.003	0.03	0.10	-	<0.001
1/DCPI	<0.001	<0.001	<0.001	<0.001	<0.001	0.22	0.38	0.10	0.42	0.68	<0.001	-

Legend: DCPI – Dynamic cone penetration index, γ_d – Dry unit weight, w – water content, PI – Plasticity index, LL – Liquid limit, #200 – Percent passing #200 sieve, %Silt – Percentage of silt, and %Clay – Percentage of clay

Table 11
A correlation matrix for the DCP test results (r-value)

	γ_d	w	M_r	DCPI	γ_d /w	#200	%Silt	%Clay	LL	PI	Log (DCPI)	1/DCPI
γ_d	1.00	-0.89	0.42	-0.49	0.75	-0.52	0.10	-0.45	-0.49	-0.42	-0.43	0.34
w	-0.89	1.00	-0.48	0.50	-0.86	0.49	-0.11	0.44	0.48	0.43	0.45	0.36
M_r	0.42	-0.48	1.00	-0.76	0.56	-0.14	0.08	-0.27	-0.18	-0.13	-0.85	0.87
DCPI	-0.49	0.50	-0.76	1.00	-0.42	0.15	-0.004	-0.10	-0.24	0.29	0.96	-0.85
γ_d /w	0.75	-0.86	0.56	-0.42	1.00	-0.62	-0.03	-0.40	-0.47	-0.42	-0.39	0.33
-# 200	-0.52	0.49	-0.14	0.15	-0.62	1.00	0.29	0.40	0.46	0.37	0.14	-0.13
%Silt	0.10	-0.11	0.08	-0.004	-0.03	0.29	1.00	-0.76	-0.60	-0.64	-0.22	0.09
%Clay	-0.45	0.44	-0.27	-0.10	-0.40	0.40	-0.76	1.00	0.88	0.86	-0.31	-0.17
LL	-0.49	0.48	-0.18	-0.24	-0.47	0.46	-0.60	0.88	1.00	0.95	0.23	-0.09
PI	-0.42	0.43	-0.13	0.29	-0.42	0.37	-0.64	0.86	0.95	1.00	0.17	-0.04
Log (DCPI)	-0.43	0.45	-0.85	0.96	-0.39	0.14	-0.22	0.31	0.23	0.17	1.00	-0.97
1/DCPI	0.34	0.36	0.87	-0.85	0.33	-0.13	0.09	-0.17	-0.09	-0.04	-0.97	1.00

Legend: DCPI – Dynamic cone penetration index, γ_d – Dry unit weight, w – water content, PI – Plasticity index, LL – Liquid limit, #200 – Percent passing sieve #200, %Silt – Percentage of silt, and %Clay – Percentage of clay

Tables 10 and 11 present the correlation coefficient matrix of all variables for this study. It is noted that the best correlation was found between the M_r and 1/DCPI (r = 0.87, p-value < 0.001). In addition, γ_d, w and γ_d/w were found to have a significant relation with M_r. Based on this result, the 1/DCPI, γ_d, w, and γ_d/w variables were further included in the stepwise selection analysis.

Table 12 presents a summary of the results of selection analysis. It is noted that the best prediction model should include only $1/DCPI^{1.46}$ and $1/w^{1.27}$ variables. In addition, $1/DCPI^{1.46}$ variable had a much higher partial R-square than the $1/w^{1.27}$ variable, which suggests that it has a greater influence on the model prediction. To demonstrate the effectiveness of the selection analysis, a multiple regression analysis was conducted on a model that includes $1/DCPI^{1.46}$, γ_d, and $1/w^{1.27}$ as independent variables. Table 13 presents the results of the analysis. It can be noted that $1/DCPI^{1.46}$ and $1/w^{1.27}$ are the only significant variables ($Pt < 0.05$); this is compatible with results of the variable selection analysis.

A simple linear regression analysis was conducted to develop a model that directly predicts the laboratory measured M_r using the 1/DCPI value. The results of this analysis yielded the model shown in equation (11), which will be referred to as the direct model. The model had a coefficient of determination, R^2, with a value of 0.9 and root mean square error, RMSE, with a value of 0.88 ksi. Figure 10 illustrates the results of regression analysis. It is observed that the proposed model fits well the data. Figure 10 also shows the 95 percent prediction interval. The 95 percent prediction interval is considered as a measure of the accuracy of the M_r values predicted using the model developed. It is noted that 95 percent of the data points fall within the boundaries of the interval.

$$M_r = \frac{151.8}{(DCPI)^{1.096}} \tag{11}$$

where,

M_r = resilient modulus (ksi), and

DCPI = dynamic cone penetration index (mm/blow).

In the absence of uniform soil properties along a soil layer, a direct relationship between the resilient modulus and DCPI is useful. A correlation among resilient modulus, soil properties, and DCPI may also be useful in examining the effect of soil properties on the DCPI predicted M_r values. Therefore, a multiple regression analysis was also conducted to develop a model that predicts laboratory measured M_r using the 1/DCPI and the physical properties of the tested soils, which will be hereafter referred to as the soil property model. The independent variables that were used in the multiple regression analysis were $1/DCPI^{1.46}$ and $1/w^{1.27}$, which were selected based on the stepwise selection analysis (Table 12). Table 14 shows the results of the multiple regression analysis. It is noted that both variables ($1/DCPI^{1.46}$ and $1/w^{1.27}$) are significant at 95 percent confidence level. In addition, those variables have variance inflation factor (VIF) values close to 1, which indicate that these variables are not collinear. Figure 11 presents the residual plot of the DCP – soil property model. No distinct pattern among the residuals exists; such rules out the model heteroscedasticity.

Table 12

Summary of stepwise selection

Variable Entered	Variable Removed	Number of Variables In	Partial R-Square	Model R-Square	F Value	Pr > F
$1/ DCPI^{1.46}$		1	0.7878	0.7878	81.3398	<0.0001
$1/w^{1.27}$		2	0.0905	0.8783	11.9417	<0.0001

Table 13

Summary of multiple regression analysis for variable selection

Variable	Parameter Estimate	t Value	Pr > |t|
Intercept	1.26	1.57	0.1211
$1/ DCPI^{1.46}$	295.63	20.74	<.0001
γ_d	-0.00910	-0.91	0.3642
$1/w^{1.27}$	97.14	7.05	<.0001

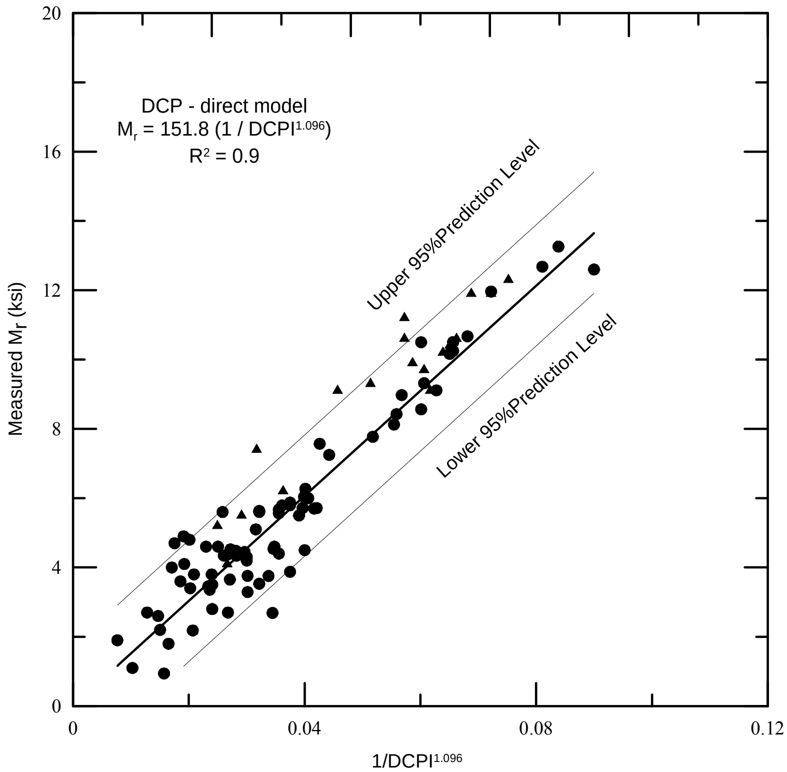

Figure 10
Variation of laboratory measured M_r with 1/DCPI

Table 14
Results of analysis of DCP – soil property model

Variable	DF	parameter estimate	t Value	Pr > |t|	standardized estimate	VIF
Intercept	1	0.56	2.18	0.0321	0	0
$1/\,DCPI^{1.46}$	1	293.20	20.97	<.0001	0.81	1.1
$1/w^{1.27}$	1	89.90	7.98	<.0001	0.31	1.1

$$M_r = 0.56 + 293.2\left(\frac{1}{DCPI^{1.46}}\right) + 89.9\left(\frac{1}{w^{1.27}}\right)$$

where,
M_r – Resilient modulus (ksi),
DCPI – Dynamic cone penetration index (mm/blow), and
w – Water content (%).

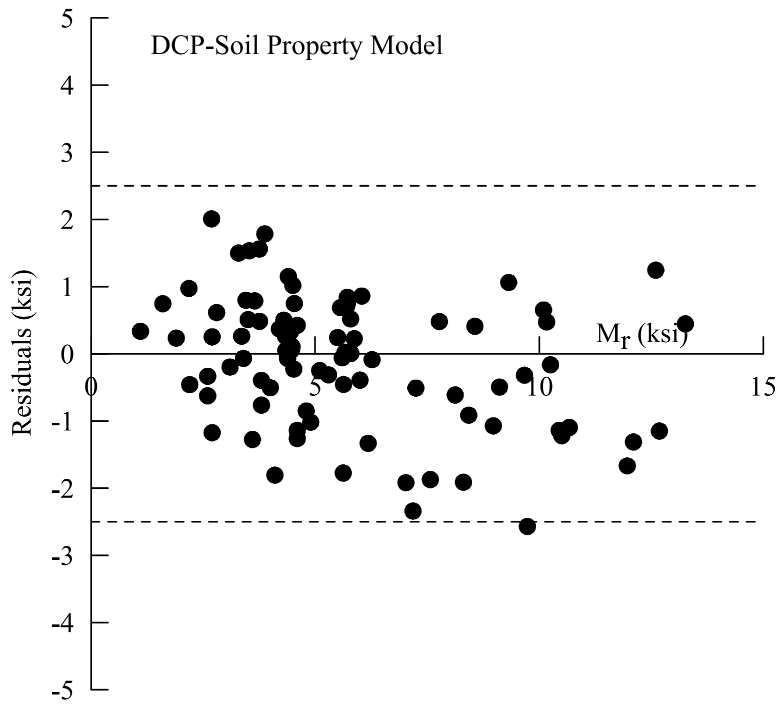

Figure 11
Residuals from DCP – soil property model

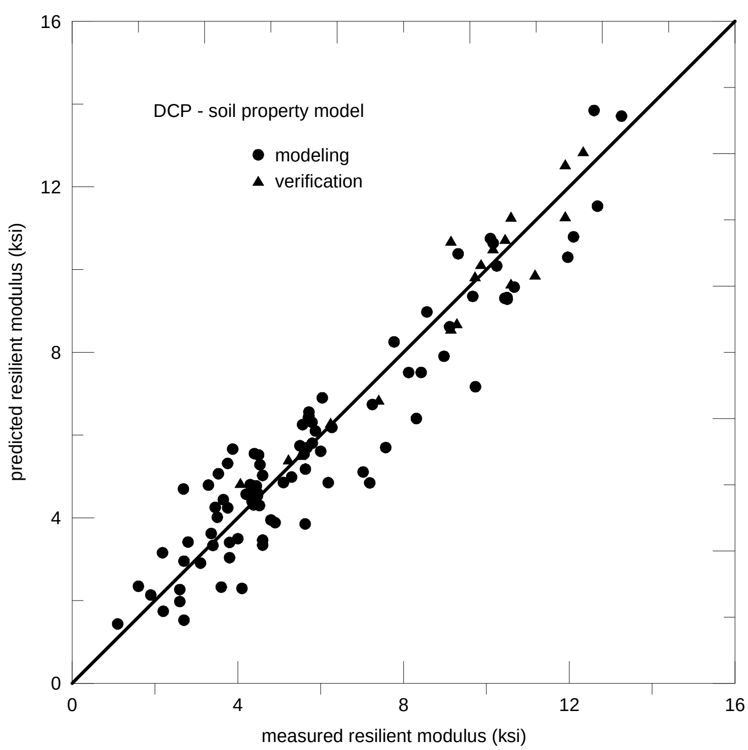

Figure 12
Laboratory measured M_r vs. values predicted from DCP – soil property model

Figure 12 shows the M_r predicted by the DCP-soil property model versus the M_r measured in the laboratory. It is observed that a good agreement was obtained between the predicted and measured values with (R^2=0.92 and RMSE=0.86). Furthermore, the model was able to provide a good prediction of the data obtained from a study reported by George et al. *[13]* that was not used in the development of the model.

Development of M_r Prediction Models for Cohesive Soils from GeoGauge Test Results

Similar to the previous section, regression analyses were conducted on the GeoGauge and M_r test results using the Statistical Analysis System (SAS) program to develop models that predict the resilient modulus of cohesive soils from the GeoGauge test results. The E_{geo} and M_r results shown in Table 15 were used to develop the models. The ranges of variables used in the regression analyses are presented in Table 16.

Table 15
GeoGauge and LFWD test results of cohesive soils

Soil ID	E_{geo} (ksi)	CV (%)	Std. (ksi)	E_{lfwd} (ksi)	CV (%)	Std. (ksi)
Clay-1	25.2	8.9	2.2	26.5	10.4	2.8
Clay-2	26.0	11.1	2.9	NA	NA	NA
Clay-3	19.8	9.7	1.9	7.6	19.7	1.5
Clay-4	22.4	8.7	2.0	19.6	46	0.9
Clay-5	11.6	5.7	0.7	7.1	19.4	1.4
Clay-6	34.9	8.6	3.0	45.7	12.5	5.7
Clay-7	23.6	21	4.9	33.2	33.5	10.5
Clayey Silt-1	8.2	15.5	1.3	4.6	13.9	0.6
Clayey Silt-2	9.7	4.3	0.4	7.2	17.1	1.2
Clayey Silt-3	2.4	11.4	0.3	4.1	46.3	1.9
Clayey Silt(ALF)	11.3	4.3	0.5	5.2	12.1	0.6
LA-182	7.9	2.4	0.2	5.4	20.6	1.1
US-61	11.6	4.2		10.1	15.8	1.6

Legend: NA – Not available, E_{geo} – Modulus from GeoGauge, E_{lfwd} – Modulus from Light falling weight deflectometer, CV – Coefficient of variation, Std. – Standard deviation

Table 16
Ranges of variables for cohesive materials

Symbol used for the variable	Description	Range
M_r	Measured laboratory resilient Modulus in (ksi)	5.6 - 12.1
E_{geo}	Measured Geogauge modulus (ksi)	2.4 - 26.0
PI	Plasticity Index, %	4 - 15
γ_d	Dry unit weight (pcf)	96.4 - 113.4
w	Water content (%)	8.5 - 20.9
LL	Liquid Limit (%)	22 - 31
%Silt	Percentage of silt (%)	28 - 72
%Clay	Percentage of clay (%)	14 - 28
#200	Percent passing #200 sieve	42 - 91

The possible linear correlations between the dependent variable M_r and each of the independent variables, such as E_{geo}, γ_d, w, γ_d/w, PI, LL, percent passing #200 sieve (#200), percentage of silt (%Silt), and percentage of clay (%Clay), were considered. Figure 13 presents the scatter plot between the dependent variable and independent variables. Figure 13a shows the variation of M_r with the GeoGauge test results. As the E_{geo} increases, M_r increases. This implies that soil strength increases as the E_{geo} increases. Therefore, a linear correlation between the E_{geo} and M_r may exist. As expected, a positive linear correlation exists between M_r and γ_d (Figure 13b). As shown in Figure 13c, a negative relationship between M_r and w exists, which is expected. Figure 13d shows the variation of M_r with the γ_d/w. As the γ_d/w increases, M_r increases with a decreasing slope until reaching a peak value, then decreases thereafter. The soil strength increases with a decreasing slope as the γ_d/w increases. These results indicate that a correlation between M_r and each of γ_d and w may exist. The correlation coefficient matrix for the different variables investigated is presented in Table 17. The best linear correlation in this table was observed between the M_r and E_{geo} (r = 0.76).

Table 18 presents results of the stepwise selection procedure. Considering the highest coefficient of determination (R^2) and the lowest square root of the mean square for error (RMSE), it is noted that the best direct prediction model was obtained when having $E_{geo}^{1.54}$ as the independent variable, while the best soil property model included $E_{geo}^{0.8}$ and $1/w^{0.78}$.

Table 17
A correlation matrix for the GeoGauge test results (r-value)

Variables	M_R	E_{GEO}	LL	PI	γ_d	w
M_R	1	0.76	0.78	0.79	0.68	-0.76
E_{GEO}	0.76	1	0.67	0.78	0.71	-0.73
LL	0.78	0.67	1	0.92	0.47	-0.80
PI	0.79	0.78	0.92	1	0.52	-0.85
γ_d	0.68	0.71	0.47	0.52	1	-0.33
w	-0.76	-0.73	-0.80	-0.85	-0.33	1

Legend: E_{geo} – Modulus from GeoGauge, γ_d – Dry unit weight, w – water content, LL – Liquid limit, and PI – Plasticity index

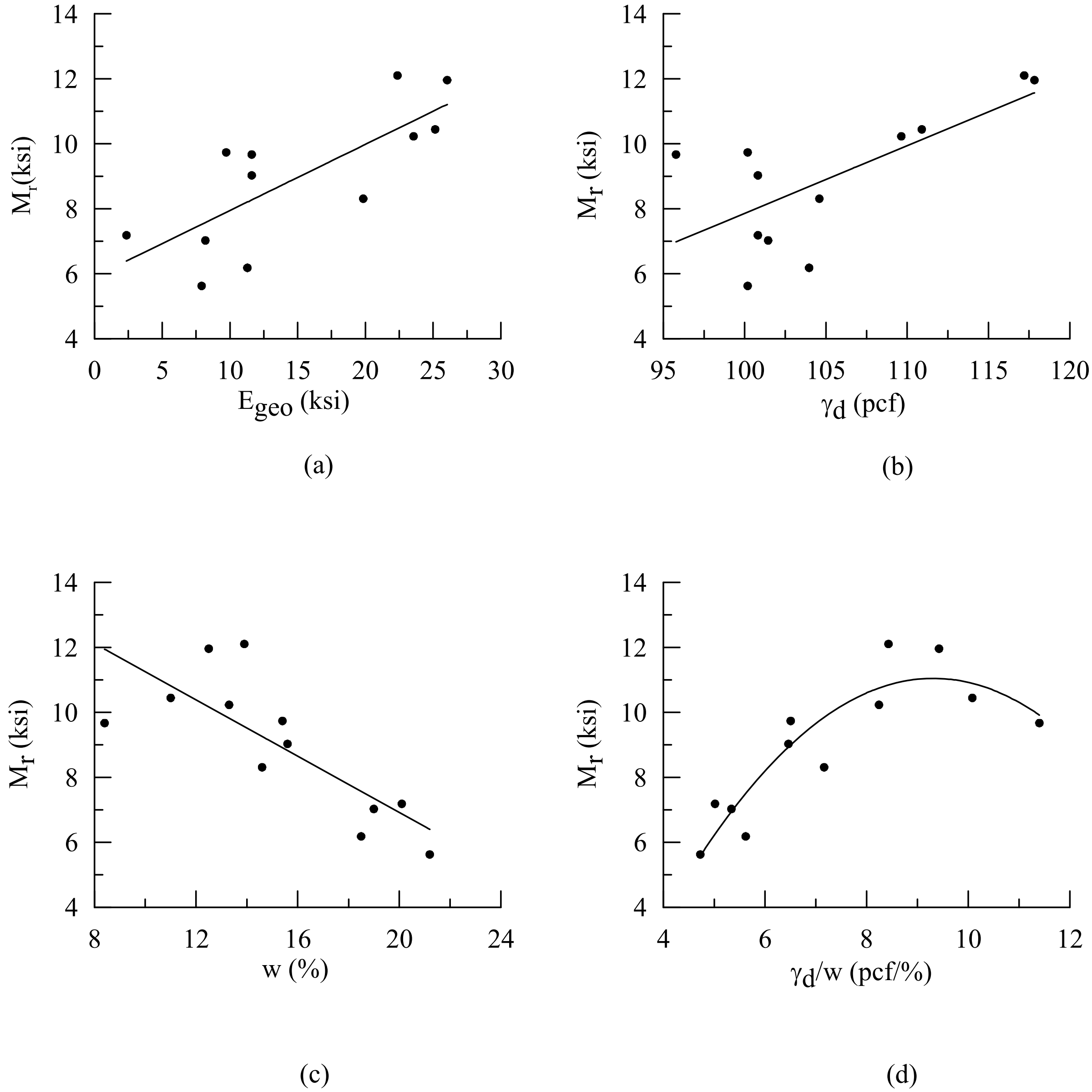

Figure 13
Variation of resilient modulus with (a) Egeo (b) γ_d (c) w (d) γ_d/w

Table 18
Selections of the GeoGauge model parameters

Model parameters	*RMSE* (ksi)	*R^2*
$M_r, E_{geo}^{1.54}$	1.44	0.59
$M_r, \frac{E_{geo}^{0.53}}{w}, (\gamma_d)$	1.23	0.70
$M_r, \frac{E_{geo}}{w}, (\gamma_d)$	1.28	0.67
$\mathrm{M_r}, \frac{E_{\mathrm{geo}}^{0.8}}{\mathrm{w}^{0.78}}$	1.22	0.72
$M_r, E_{geo}, (\gamma_d)$	1.44	0.59
$M_r, E_{geo}^{0.15}, \left(\frac{\gamma_d}{w}\right), PI$	1.34	0.68

A simple linear regression analysis was conducted to develop a model that directly predicts the laboratory measured M_r from the $E_{geo}^{1.54}$ value. The results of the analysis are presented in Table 19 and equation (12). The model had a coefficient of determination, R^2, value of 0.59 and root mean square error, RMSE, value of 1.44 ksi. The ratio of the standard deviation for the error to the standard deviation of the measured M_r (S_e/S_y) was also 0.68. Figure 14 illustrates the results of the regression analysis. It is observed that the data points are widely scattered about the model line.

$$M_r = 6.74 + 0.03 E_{geo}^{1.54} \tag{12}$$

where,
M_r = resilient modulus (ksi), and
E_{geo} = modulus from GeoGauge test (ksi).

A multiple regression analysis was also conducted to develop a soil property model that predicts laboratory measured M_r from the E_{geo} and the physical properties of the tested soils. The independent variables that were used in the multiple regression analysis were $E_{geo}^{0.8}$ and $1/w^{0.78}$, which were selected based on the selection analysis (Table 18). The results of this analysis are presented in Table 20 and equation (13). The soil property model had R^2 and

RMSE of 0.72 and 1.22, respectively. The results of the measured M_r and those predicted using the model in equation (13) are shown in Figure 15. It is noted that data points are much less scattered about the model line compared to those in Figure 14 showing that the soil property model yielded a better prediction of the laboratory measured M_r. Finally, Figure 16 presents the residual plot of the GeoGauge-soil property model. There is no distinct pattern among the residuals, which rules out the model heteroscedasticity.

$$M_r = -2.023 + 0.027\left(E_{geo}{}^{0.8}\right) + 87.24\left(\frac{1}{w^{0.78}}\right) \qquad (13)$$

where,
M_r = resilient modulus (ksi),
E_{geo} = modulus from GeoGauge test (ksi), and
w = water content (%).

Table 19
Results of the regression analysis for the GeoGauge – direct model

Model	Parameter estimated	Pr> F (p-value)	Pr> | t | (p-value)
M_r, E_{geo}	Model	0.0038	-
	E_{geo}	-	0.0038

Table 20
Results of the regression analysis for the Geogauge – soil property model

Model	Parameter estimated	Pr> F (p-value)	Pr> | t | (p-value)
M_r, $E_{geo}{}^{0.8}$, $1/w^{0.78}$	Model	< 0.0001	-
	$E_{geo}{}^{0.8}$	-	0.006
	$1/w^{0.78}$	-	< 0.001

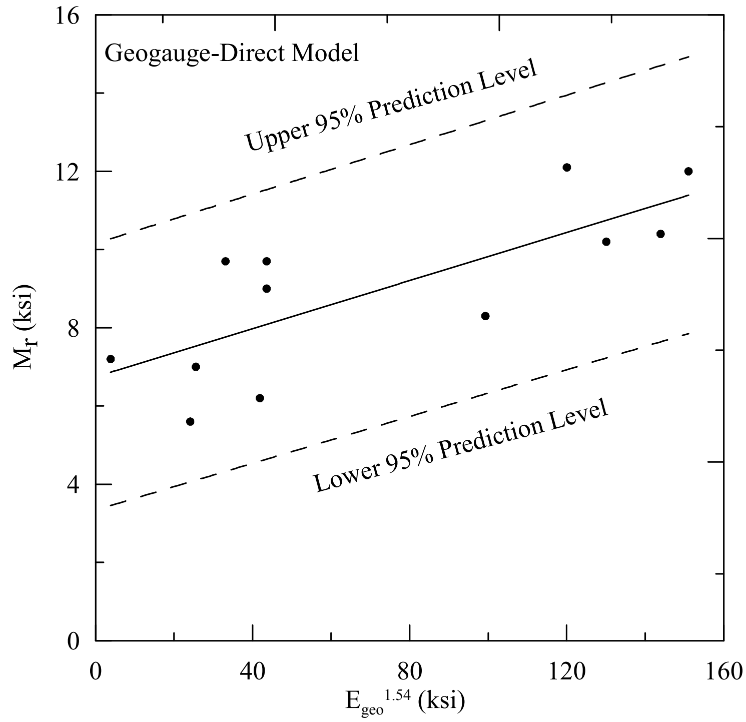

Figure 14
Predictions from the GeoGauge – direct model

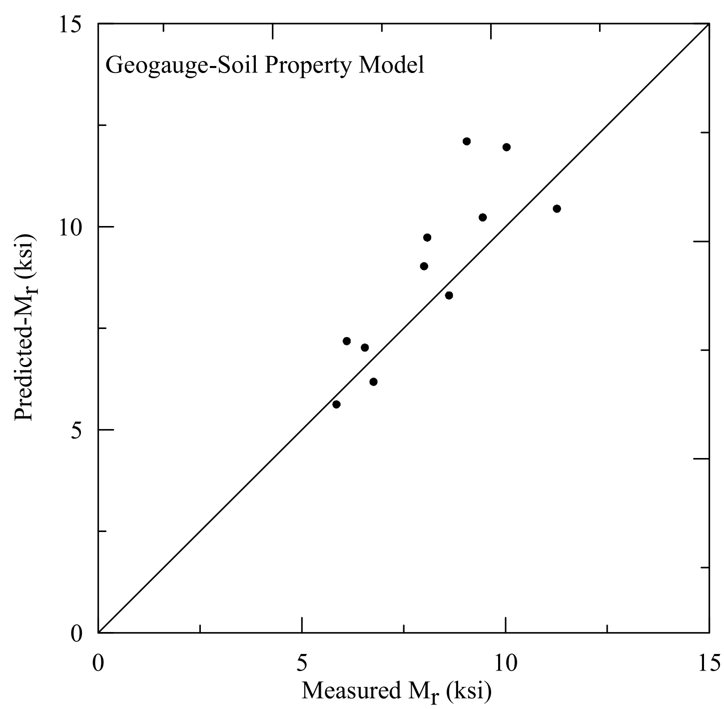

Figure 15
Predictions from the GeoGauge – soil property model

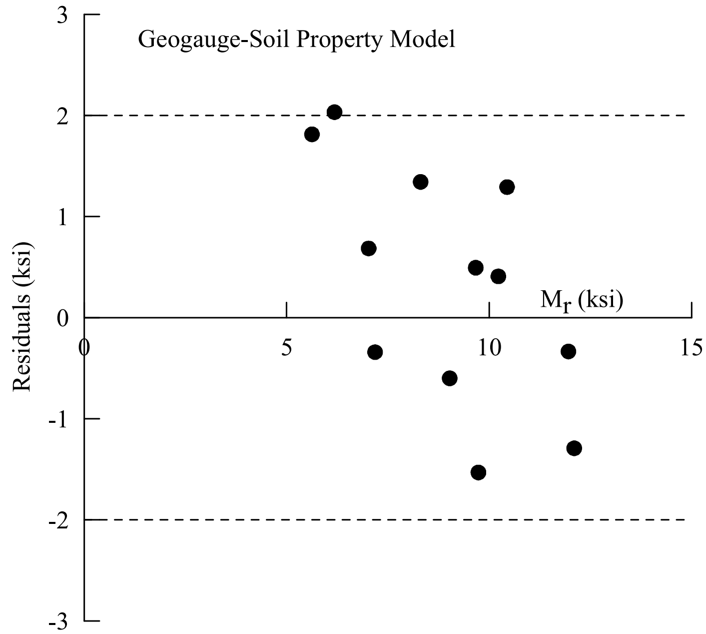

Figure 16
Residuals from GeoGauge – soil property model

Development of M_r Prediction Models for Cohesive Soils from LFWD Test Results

Regression analyses were also conducted on the LFWD and M_r test results to develop models that predict the resilient modulus of cohesive soils from the LFWD test data. The E_{lfwd} and M_r results were used to develop the model and are shown in Table 15. The ranges of variables are presented in Table 21.

The possible linear correlation between the dependent variables M_r and E_{lfwd} was examined. Figure 17 shows the variation of M_r with the LFWD test results. As the E_{lfwd} increases, M_r increases indicating that soil strength increases as the E_{lfwd} increases. However, the increase is not linear. Therefore, Table 22 shows the possible linear correlation matrix between M_r and the other variable investigated. It is noted that, in general, better linear correlation was observed between M_r and the tested soils' physical properties, compared to those between M_r and $E_{lfwd.}$

Table 23 presents results of the stepwise selection procedure. It is noted that the best direct prediction model as measured by the R^2 and RMSE was obtained when having $E_{lfwd}^{0.18}$ as the independent variable while the best soil property model included $E_{lfwd}^{0.2}$ and 1/w.

Table 21
Ranges of variables for cohesive materials

Symbol used for the variable	Description	Range
M_r	Measured laboratory resilient modulus in (ksi)	5.6-12.1
E_{lfwd}	Measured LFWD modulus (ksi)	4.1-45.7
PI	Plasticity index (%)	4-15
γ_d	Dry unit weight (pcf)	96.4-113.4
w	Water content (%)	8.5-20.9
LL	Liquid limit (%)	22-31
%Silt	Percentage of silt (%)	28-72
%Clay	Percentage of clay (%)	14-28
#200	Percent passing #200 sieve	42-91

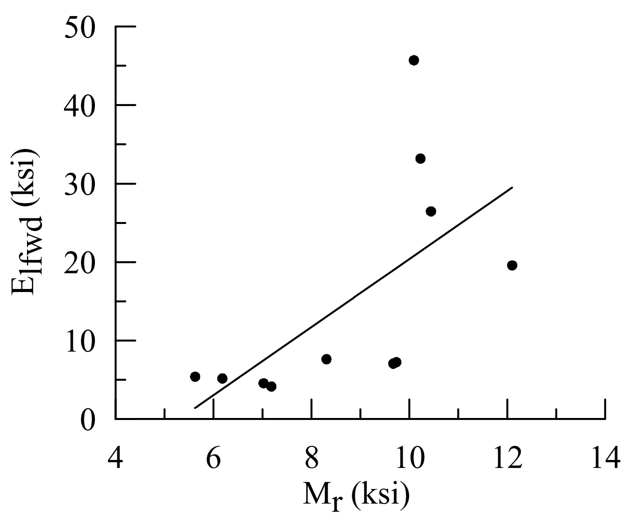

Figure 17
Variation of resilient modulus with E_{lfwd}

Table 22
A correlation matrix for the LFWD test results (r-value)

Variables	M_R	E_{LFWD}	LL	PI	γ_d	w%
M_R	1	0.61	0.78	0.79	0.68	-0.76
E_{LFWD}	0.61	1	0.53	0.63	0.60	-0.64
LL	0.78	0.53	1	0.92	0.47	-0.80
PI	0.79	0.63	0.92	1	0.52	-0.85
γ_d	0.68	0.60	0.47	0.52	1	-0.33
w%	-0.76	-0.64	-0.80	-0.85	-0.33	1

Table 23
Selections of the LFWD model parameters

Model parameters	RMSE (ksi)	R^2
$M_r, E_{lfwd}^{0.18}$	1.33	0.54
$M_r, \left(\frac{E_{lfwd}^{0.17}}{w}\right), \gamma_d$	1.28	0.61
$M_r, E_{lfwd}^{0.2}, 1/w$	1.05	0.7
M_r, E_{lfwd}	1.61	0.38
$M_r, E_{lfwd}, \frac{\gamma_d}{w}$	1.43	0.56
M_r, E_{lfwd}, γ_d	1.58	0.47
$M_r, E_{lfwd}, \frac{\gamma_d}{w}, PI$	1.95	0.18

A linear regression analysis was performed on the data to develop a model that directly predicts the laboratory measured M_r from the $E_{lfwd}^{0.18}$. The results of the analysis are presented in Table 24 and equation (14). The model had a coefficient of determination, R^2, with a value of 0.54 and RMSE with a value of 1.33 ksi. The ratio of the standard deviation for the error to the standard deviation of the measured M_r (S_e/S_y) was also 0.74. Figure 18 illustrates the prediction of the LFWD direct model. It is observed that the data points are widely scattered about the model line.

$$M_r = 5.70 E_{lfwd}^{0.18} \tag{14}$$

where,
M_r = resilient modulus (ksi), and

E_{lfwd}= modulus from LFWD test (ksi).

A multiple regression analysis was also conducted to develop a soil property model that predicts laboratory measured M_r from the E_{lfwd} along with the physical properties of the tested soils. The independent variables that were used in the multiple regression analysis were $E_{lfwd}^{0.2}$ and 1/w, which were chosen based on the selection analysis (Table 23). The results of this analysis are presented in Table 25 and equation (15). The soil property model had R^2 and RMSE values of 0.70 and 1.05, respectively. Figure 19 illustrates the prediction of the LFWD soil property model. It is observed the prediction of the model is enhanced when including the physical properties of the tested soils. Figure 20 presents the residual plot of LFWD – soil property model. There is no distinct pattern among the residuals, which rules out the model heteroscedasticity.

$$M_r = 1.63 + 2.7\left(E_{lfwd}^{0.2}\right) + 35.17\left(\frac{1}{w}\right) \tag{15}$$

where,
M_r = resilient modulus (ksi),
E_{lfwd} = modulus from LFWD test (ksi), and
w = water content (%).

Table 24
Results of the regression analysis for the LFWD – direct model

Model	Parameter estimated	Pr> F (p-value)	Pr> | t | (p-value)
$M_r, E_{lfwd}^{0.18}$	Model	0.0001	-
	E_{lfwd}	-	0.0001

Table 25
Results of the regression analysis for the LFWD – soil property model

Model	Parameter estimated	Pr> F (p-value)	Pr> | t | (p-value)
$M_r, \left(E_{lfwd}^{0.2}\right), \left(\frac{1}{w}\right)$	Model	< 0.0001	-
	$E_{lfwd}^{0.2}$	-	0.0477
	1/w	-	0.0385

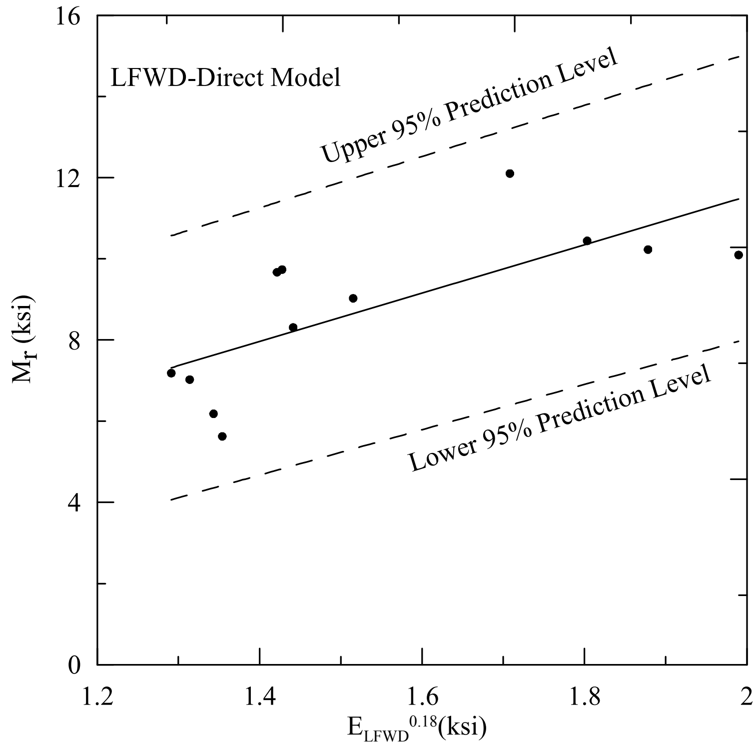

Figure 18
Predictions from the LFWD-direct model

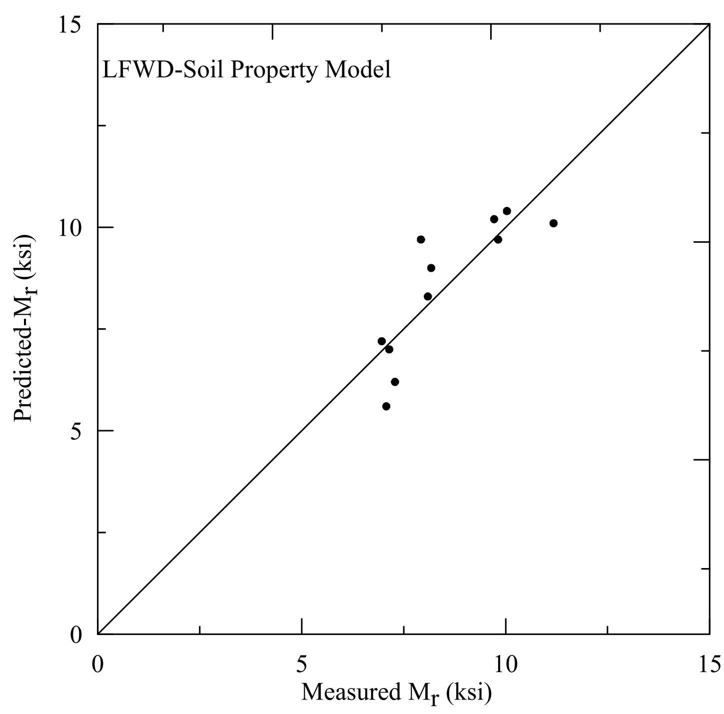

Figure 19
Predictions from the LFWD-soil property model

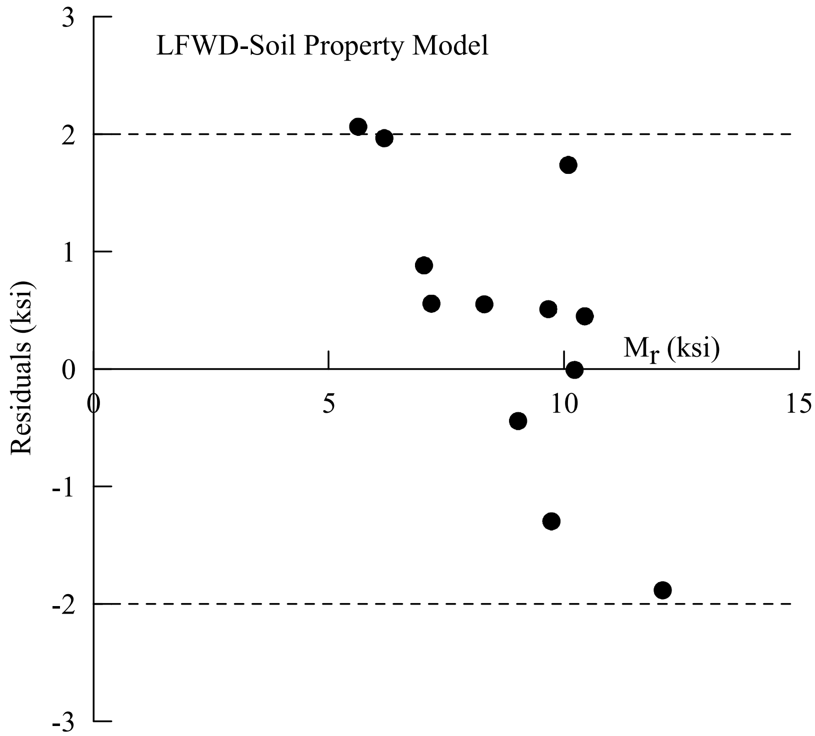

Figure 20
Residuals from LFWD-soil property model

Development of M_r Prediction Models for Granular Soils from DCP Test Results

Regression analyses were performed on the DCP and M_r test results using the SAS program to develop models that predict the resilient modulus of granular materials from the DCP test data. The DCPI and M_r results shown in Table 26 were used to develop the different models. The ranges of variables are presented in Table 27.

The possible linear correlation between the dependent variable M_r and the independent variables was considered. Figure 21 shows the variation of M_r with the DCPI test results. As the DCPI decreases, M_r increases, indicating that soil stiffness increases as the DCPI decreases. Therefore, there may be a linear correlation between the DCPI and M_r. A correlation matrix of the different variables investigated in this study is shown in Table 28. It is noted the best linear correlation was observed between the DCPI and M_r.

Table 29 presents a summary of the results of stepwise selection analysis. It is noted that the best soil property model should include only $1/DCPI^{0.15}$ and the percent passing #4 sieve (P_4) variables. In addition, the $1/DCPI^{0.15}$ had a higher partial R^2 than the passing #4 sieve, indicating that $1/DCPI^{0.15}$ has a higher significance in the model.

Table 26
Resilient modulus and DCP test results of granular materials

Type of Material	Soil ID	Location	M_r (ksi)	CV (%)	Std. (ksi)	DCPI (mm/blow)
Crushed Limestone	CL1-1	Field	28.6	3	0.9	43.8
	CL1-2	Field	30.9	4	1.2	23.1
	CL1-3	Field	29.2	1	0.3	9.8
	CL1-4	Lab	27.6	4	1.1	13.7
	CL2	Lab	35.7	17	6.1	8.8
Sand	Sand-1	Lab	29.5	7	2.1	25.5
	Sand-2	Lab	22.2	16	3.6	27.4
	Sand-3	Lab	22.2	16	3.6	61.0
	Sand-4	Field	20.8	3	0.6	66.7
	Sand-5	Field	26.1	10	2.7	23.4
	Sand-6	Field	26.1	10	2.7	18.8
Recycled Asphalt Pavement	Rap-1	Field	26.1	3	0.8	30.3
	Rap-2	Field	34.5	3	1.0	16.1
	Rap-3	Field	43.3	3	1.3	10.0
	Rap-4	Field	35.8	14	5.0	9.0

Legend: NA – Not available, DCPI – DCP penetration index, E_{geo} – Modulus from GeoGauge, E_{lfwd} – Modulus from Light falling weight deflectometer, M_r – Measured Resilient modulus, CV – Coefficient of variation, Std. – Standard deviation, Lab – Laboratory

Table 27
Ranges of variables for granular base materials

Type of Variable	Symbol used for the variable	Description	Range
Dependent	M_r	Measured laboratory resilient Modulus in ksi	20.8 -43.3
Independent or Explanatory	DCPI	Measured DCP index in mm/blow	8.8 - 66.7
	P_{200} or $P_{0.075}$	Percent passing 0.075 mm sieve (#200)	0.2 - 13
	P_4 or $P_{4.75}$	Percent passing 4.75 mm sieve (#4)	50 - 99
	γ_d	Dry unit weight (pcf)	99.6 - 132.9
	w	Water content (%)	2 -13.3

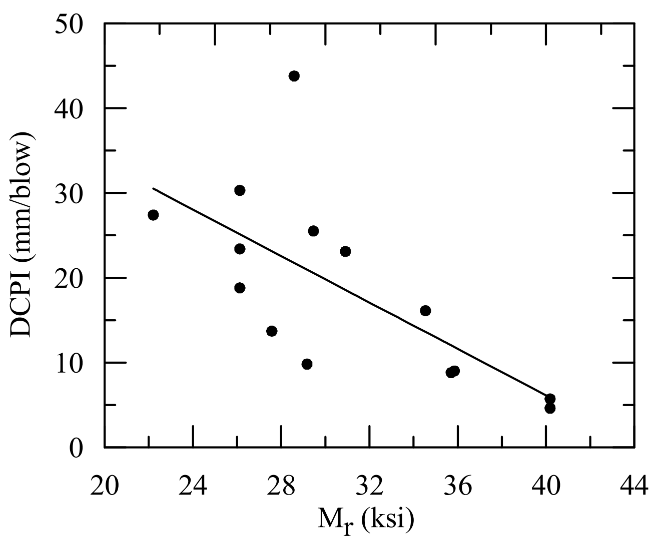

Figure 21
Variation of resilient modulus with DCPI

Table 28
A correlation matrix for the DCP test results (r-value)

Variables	M_r	DCPI	P_{200}	P_4	γ_d	w
M_r	1	-0.73	0.38	-0.71	0.60	0.54
DCPI	-0.73	1	-0.38	0.63	-0.58	-0.43
P_{200}	0.38	-0.38	1	-0.69	0.80	-0.06
P_4	-0.71	0.63	-0.69	1	-0.66	-0.48
γ_d	0.60	-0.58	0.80	-0.66	1	-0.05
w	0.54	-0.43	-0.06	-0.48	-0.05	1

Table 29
Selections of the DCP model parameters

Model parameters	RMSE (ksi)	R^2
$M_r, \frac{1}{DCPI^{0.23}}$	2.94	0.77
$M_r, \frac{1}{DCPI^{0.15}}, p_4$	2.70	0.82
$M_r, \frac{1}{DCPI^{0.21}}, \frac{\gamma_d}{w}$	2.96	0.78
$M_r, \frac{1}{DCPI^{0.22}}, p_{200}$	3.02	0.77
$M_r, \frac{1}{DCPI^{0.20}}, \frac{\gamma_d}{w}, p_{200}$	3.04	0.78
$M_r, Log(DCPI)$	3.15	0.75

A linear regression analysis was first conducted to develop a model that predicts the laboratory measured M_r from the $1/DCPI^{0.23}$ value. The results of the analysis (Table 30) yielded the model shown in equation (16). The model had an R^2 value of 0.77 and an RMSE value of 2.94 ksi. Figure 22 illustrates the results of regression analysis. It is observed that the proposed model fits the data well. It is also noted that all of the data points fall within the boundaries of this 95 percent prediction interval.

$$M_r = \frac{56.73}{DCPI^{0.23}} \tag{16}$$

Multiple regression analysis was also conducted to develop a model that predicts laboratory measured M_r from the 1/DCPI and the physical properties of the tested soils. The independent variables that were used in the multiple regression analysis were $1/DCPI^{0.15}$ and the percent passing sieve No. 4 (P_4), which were chosen based on the stepwise selection analysis (Table 29). Table 31 shows the results of the multiple regression analysis. It is noted that both variables ($1/DCPI^{0.15}$ and P_4) are significant at 95 percent confidence level. Figure 23 presents the prediction of the DCP-Material Property model. Figure 24 shows the residuals of the DCP- material property model versus the measured M_r. It is noted that there is no distinct pattern among the residuals, which rules out any possible heteroscedasticty.

$$M_r = \frac{53.74}{DCPI^{0.15}} - 0.07 p_4 \tag{17}$$

where,
M_r = resilient modulus (ksi),
DCPI = DCP index (mm/blow),
p_4 = percent passing sieve No. 4,
γ_d = dry unit weight (pcf), and
w = water content (%).

Table 30
Results of the regression analysis for the DCPI – direct model

Model	Parameter estimated	Pr> F (p-value)	Pr> | t | (p-value)
$M_r, \frac{1}{DCPI^{0.23}}$	Model	0.0001	-
	$\frac{1}{DCPI^{0.23}}$	-	0.0001

Table 31
Results of the regression analysis for the DCPI – material property model

Model	Parameter estimated	Pr> F (p-value)	Pr> | t | (p-value)
$M_r, \frac{1}{DCPI^{0.15}}, p_4$	Model	< 0.0001	-
	$\frac{1}{DCPI^{0.15}}$	-	< 0.0001
	p_4	-	< 0.0059

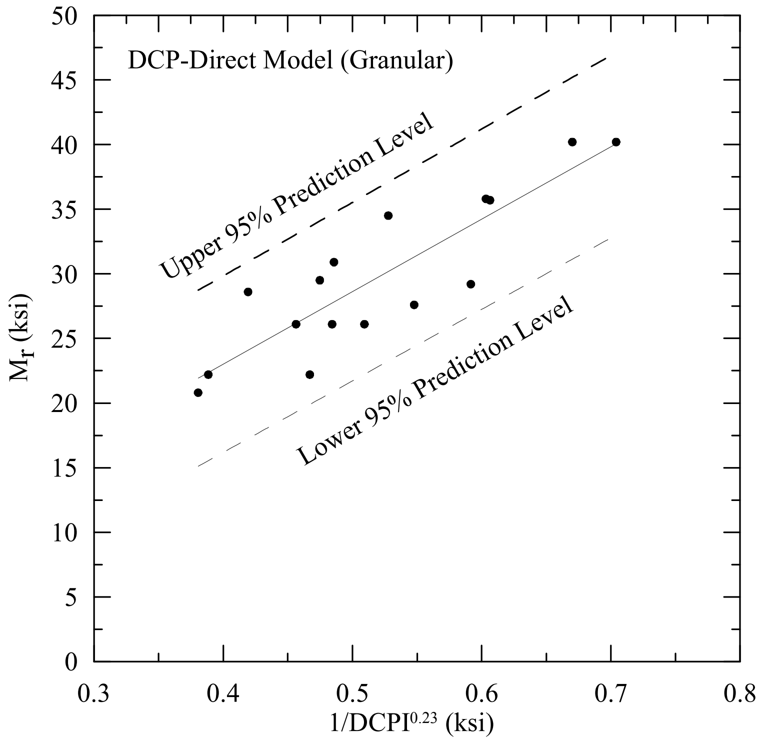

Figure 22
Predictions from the DCP – direct model

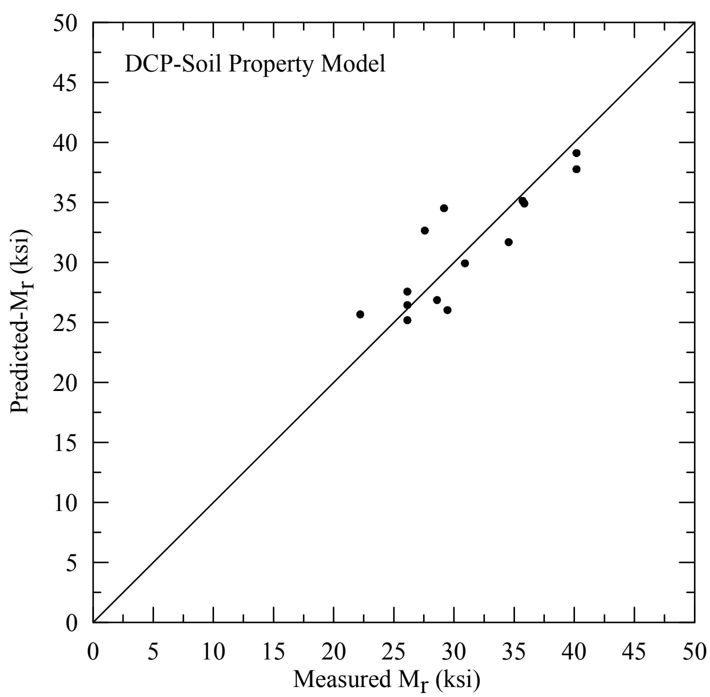

Figure 23
Predictions from the DCP – soil property model

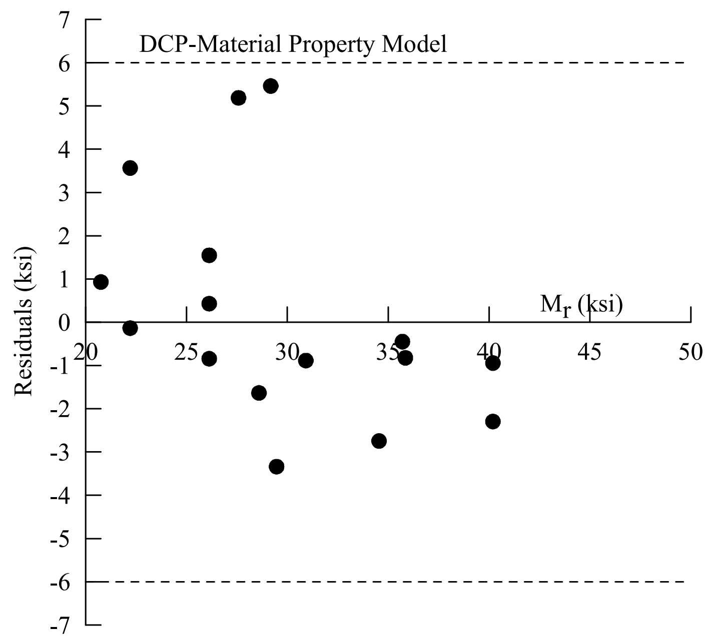

Figure 24
Residuals from DCP-material property model

Development of M_r Prediction Models for Granular Soils from GeoGauge Test Results

Regression analyses were also performed on the test results shown in Table 32 to develop models that predict the resilient modulus of granular materials from the GeoGauge test results. The ranges of different variables used in the regression analyses are presented in Table 33.

The possible linear correlation between the dependent variable M_r and E_{geo} were considered first. Figure 25 shows the variation of M_r with the GeoGauge test results. It is noted that as the E_{geo} increases, the M_r linearly increases. Therefore, there may be a linear correlation between the E_{geo} and M_r. Table 34 presents the linear correlation matrix of the different variables investigated in this study. It is noted that high coefficient of correlation was detected between E_{geo} and M_r, which confirms the results in Figure 25.

In a procedure similar to the procedure followed in developing the previous regression models, a stepwise selection analysis was conducted to select the independent variable that should be included in the direct and the material property models. Table 35 presents the results of the selection analysis. It is noted that, based on R^2 and RMSE, the best direct model should include LOG(E_{geo}) while the best material property model should have LOG(E_{geo}), p_4, and p_{200} as the independent variables.

Table 32
GeoGauge and LFWD test results of granular materials

Type of Material	Soil ID	E_{geo} (ksi)	CV (%)	Std. (ksi)	E_{lfwd} (ksi)	CV (%)	Std. (ksi)
Crushed Limestone	CL1-1	8.3	2.8	0.2	5.0	13.5	0.7
	CL1-2	10.6	4	0.4	8.3	9.3	0.8
	CL1-3	13.9	3.8	0.5	12.0	3.8	0.4
	CL1-4	22.5	3.1	0.7	10.8	17.2	1.8
	CL2	18.1	7.6	1.4	19.0	3	0.6
Sand	Sand-1	8.2	8.5	0.7	2.6	55.8	0.8
	Sand-2	7.2	5.4	0.4	5.9	13.9	0.6
	Sand-3	7.2	2.3	0.2	3.0	27.6	0.8
	Sand-4	5.9	5.4	0.3	1.8	18	0.3
	Sand-5	7.9	2.9	0.2	3.7	15.8	0.6
	Sand-6	8.5	7.5	0.6	6.1	2.3	0.1
Recycled Asphalt Pavement	Rap-1	8.3	4.2	0.3	4.2	15.9	0.7
	Rap-2	11.2	2.3	0.2	7.5	13.1	1.0
	Rap-3	18.3	5.1	0.9	16.9	4.4	0.7
	Rap-4	14.3	3.8	0.5	20.1	24.5	4.9

Legend: NA – Not available, E_{geo} – Modulus from Geogauge, E_{lfwd} – Modulus from Light falling weight deflectometer, CV – Coefficient of variation, Std. – Standard deviation

Table 33
Ranges of variables for granular base materials

Type of Variable	Symbol used for the variable	Description	Range
Dependent	M_r	Measured laboratory resilient Modulus in ksi	20.8-43.3
Independent or Explanatory	E_{geo}	Measured GeoGauge modulus in ksi	5.9-18.3
	P_{200} or $P_{0.075}$	Percent passing 0.075 mm sieve (#200)	0.2-13
	P_4 or $P_{4.75}$	Percent passing 4.75 mm sieve (#4)	50-99
	γ_d	Dry unit weight (pcf)	99.6-132.9
	w	Water content (%)	2-13.3

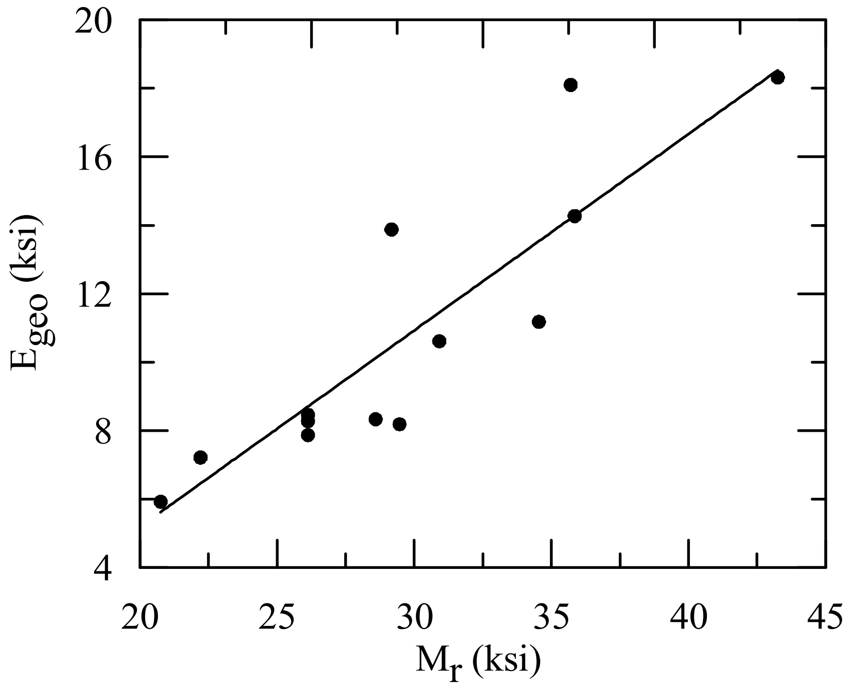

Figure 25
Variation of resilient modulus with E_{geo}

.

Table 34
A correlation matrix for the GeoGauge test results (r-value)

Variables	M_r	E_{geo}	$P_{0.075}$	$P_{4.75}$	γ_d	w
M_r	1	0.90	0.13	-0.67	0.41	0.62
E_{geo}	0.90	1	0.32	-0.69	0.59	-0.73
$P_{0.075}$	0.13	0.32	1	-0.58	0.85	-0.13
$P_{4.75}$	-0.67	-0.69	-0.58	1	-0.52	-0.69
γ_d	0.41	0.59	0.85	-0.52	1	-0.10
w	0.62	-0.73	-0.13	-0.69	-0.10	1

Table 35
Selections of the GeoGauge model parameters

Model parameters	RMSE (ksi)	R^2
$M_r, LOG(E_{geo})$	2.79	0.82
$M_r, LOG(E_{geo}), p_4, p_{200}$	2.34	0.88
$M_r, E_{geo}^{0.41}, p_4$	2.79	0.82
$M_r, LOG(E_{geo}), p_4$	2.75	0.82
$M_r, LOG(E_{geo}), p_{200}$	2.70	0.83
$M_r, E_{geo}^{0.45}, \frac{\gamma_d}{w}$	2.70	0.83

In order to develop a model that predicts the laboratory measured M_r directly from the LOG (E_{geo}), a linear regression analysis was performed on the data in Table 32. The results of the analysis are shown in Table 36, and the developed model is presented in equation (18). The model had an R^2 value of 0.82 and an RMSE value of 2.79 ksi. Figure 26 illustrates the prediction of the GeoGuage direct model regression analysis. It is observed that the proposed model fits the data well. Figure 26 also shows the 95 percent prediction interval. In addition, it is noted that all of the data points fall within the boundaries of the 95 percent prediction interval.

$$M_r = 36.68LOG(E_{geo}) - 7.21 \tag{18}$$

where,
M_r = resilient modulus (ksi), and
E_{geo} = modulus from GeoGauge test (ksi).

Multiple regression analysis was also conducted to develop a model that predicts laboratory measured M_r from the E_{geo} and the physical properties of the tested soils. The independent variables that were used in the multiple regression analysis were LOG(E_{geo}), P_{200}, and P_4, which were selected based on the stepwise selection analysis (Table 35). Table 37 shows the results of the multiple regression analysis. In addition, equation (19) presents the developed model. The model had an R^2 value of 0.88 and an RMSE value of 2.34 ksi. It is noted that all variables (LOG(E_{geo}), P_{200}, and P_4) are significant at 95 percent confidence level. However, LOG(E_{geo}) is the most significant variable. Figure 27 presents the prediction of GeoGauge-material property model. It is noted that a good agreement is obtained between measured and predicted M_r values pertaining to the model. Figure 28 shows the model residuals versus the measured M_r. It is noted that there is no distinct pattern among the residuals, ruling out the any possible heteroscedasticty.

$$M_r = 35.38LOG(E_{geo}) - 0.06p_4 - 0.39p_{200} \tag{19}$$

where,
M_r = resilient modulus (ksi),
E_{geo} = modulus from GeoGauge test (ksi),
P_4 = percent passing sieve No. 4,
P_{200} = percent passing sieve No. 200,
γ_d = dry unit weight (pcf), and
w = water content (%).

Table 36
Results of the regression analysis for the GeoGauge – direct model

Model	Parameter estimated	Pr > F (p-value)	Pr > | t | (p-value)
$M_r, LOG(E_{geo})$	Model	0.0001	-
	$LOG(E_{geo})$	-	0.0001

Table 37
Regression analysis for the GeoGauge – material property model

Model	Parameter estimated	Pr > F (p-value)	Pr > | t | (p-value)
$M_r, LOG(E_{geo}), p_4, p_{200}$	Model	< 0.0001	-
	$LOG(E_{geo})$	-	< 0.0001
	p_4	-	0.0167
	p_{200}	-	0.0357

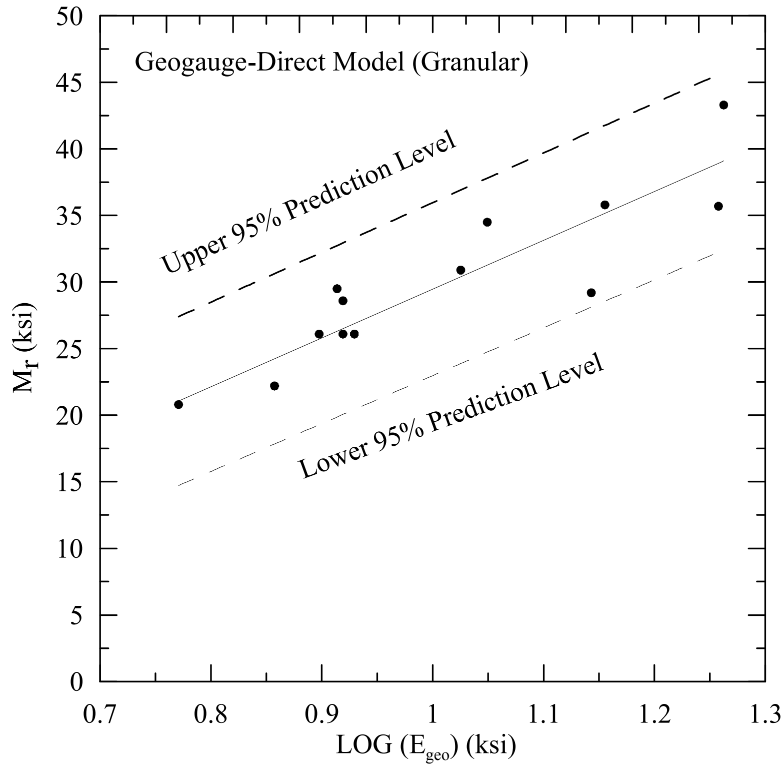

Figure 26
Predictions from the GeoGauge – direct model

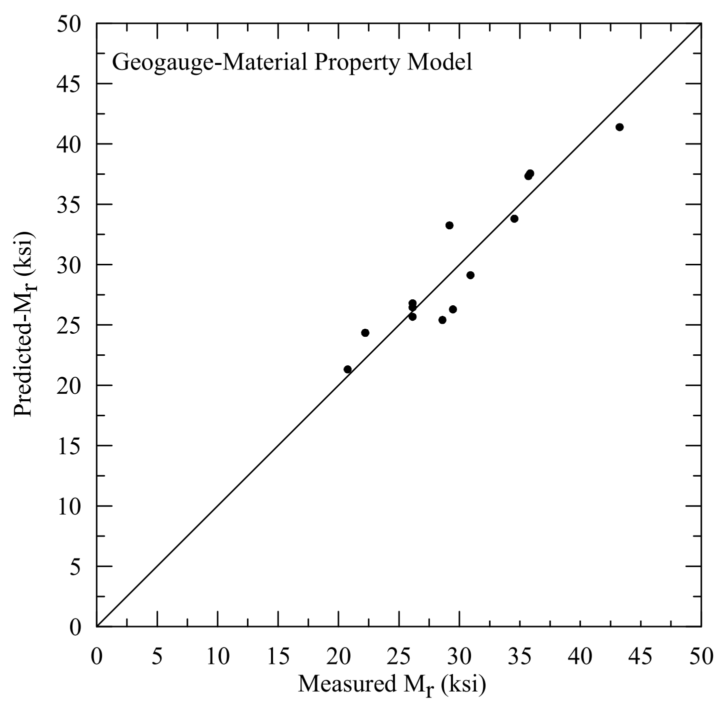

Figure 27
Predictions from the GeoGauge – material property model

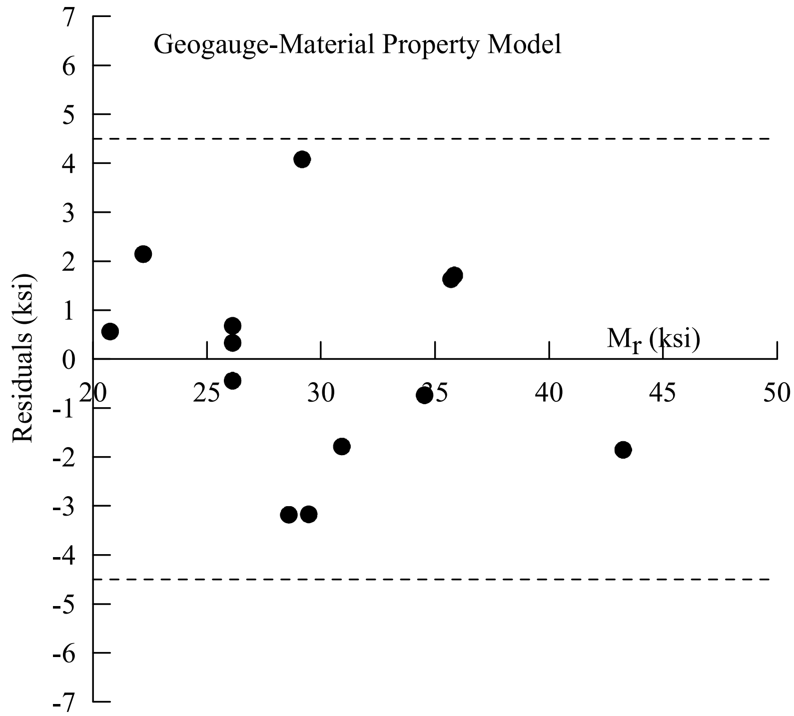

Figure 28
Residuals from GeoGauge – material property model

Development of M_r Prediction Models for Granular Soils from LFWD Test Results

Regression analyses were performed on the LFWD and M_r test results to develop models that predict the M_r of granular materials from the LFWD test data. The ranges of variables used in these analyses are presented in Table 38.

The possible linear correlation between the dependent variable M_r and E_{lfwd} was considered. Figure 29 shows the variation of M_r with the LFWD test results. It is noted that M_r increases with an increase of the E_{lfwd}. However, the relationship between M_r and E_{lfwd} is not linear. Table 39 presents the linear correlation matrix of all variables. It is noted that, of all the variables, the E_{lfwd} has the best correlation with laboratory measured M_r values.

A stepwise selection analysis was conducted to select the independent variable that should be included in the direct and the material property models. Table 40 presents the results of the analysis. It is noted that based on R^2 and RMSE, the best direct model should include $E_{lfwd}^{0.21}$, while the best material property model should have $E_{lfwd}^{0.11}$ and p_4 as the independent variables.

In order to develop a model that predicts the laboratory measured M_r directly from the $E_{lfwd}^{0.21}$, a linear regression analysis was performed on the data in Table 32. The results of this analysis are shown in Table 41, while the developed model is presented in equation (20). The model had an R^2 value of 0.70 and an RMSE value of 2.77 ksi. Figure 30 illustrates the prediction of the LFWD direct model regression analysis. It is observed that the proposed model well fits the data. Figure 30 also shows the 95 percent prediction interval. In addition, it is noted that all of the data points fall within the boundaries of this 95 percent prediction interval.

$$M_r = 18.69 E_{lfwd}^{0.21} \tag{20}$$

where,
M_r = resilient modulus (ksi), and
E_{lfwd} = modulus from LFWD test (ksi).

Multiple regression analysis was also conducted to develop a model that predicts laboratory measured M_r from the E_{lfwd} and the physical properties of the tested soils. The independent variables that were used in the multiple regression analysis were $E_{lfwd}^{0.11}$ and P_4, which were selected based on the stepwise selection analysis (Table 40). Table 42 shows the results of the multiple regression analysis. In addition, equation (21) presents the developed model. The model had an R^2 value of 0.77 and an RMSE value of 2.35 ksi. Figure 31 shows the prediction of the LFWD – material property model. It is noted that the LFWD – material property model provided a better prediction than the LFWD – direct model. Figure 32 shows the model residuals versus the measured M_r. It is noted that there is no distinct pattern among the residuals, ruling out any possible heteroscedasticty.

$$M_r = 27.48 E_{lfwd}^{0.11} - 0.08 P_4 \tag{21}$$

where,
M_r = resilient modulus (ksi),
E_{lfwd} = modulus from LFWD test (ksi),
P_4 = percent passing sieve #4,
γ_d = dry unit weight (pcf), and
w = water content (%).

Limitations of the Models

The prediction models developed in this study are only valid for the soils' types and ranges investigated. It is noted that the models developed for the granular materials were derived based on limited data points.

Table 38
Ranges of variables for granular base materials

Type of Variable	Symbol used for the variable	Description	Range
Dependent	M_r	Measured laboratory resilient modulus in ksi	20.8-43.3
Independent or Explanatory	E_{lfwd}	Measured LFWD modulus in MPa	1.8-20.1
	P_{200} or $P_{0.075}$	Percent passing 0.075 mm sieve	0.2-13
	P_4 or $P_{4.75}$	Percent passing 4.75 mm sieve	50-99
	γ_d	Dry unit weight (pcf)	99.6-134
	w	Water content (%)	2-13.3

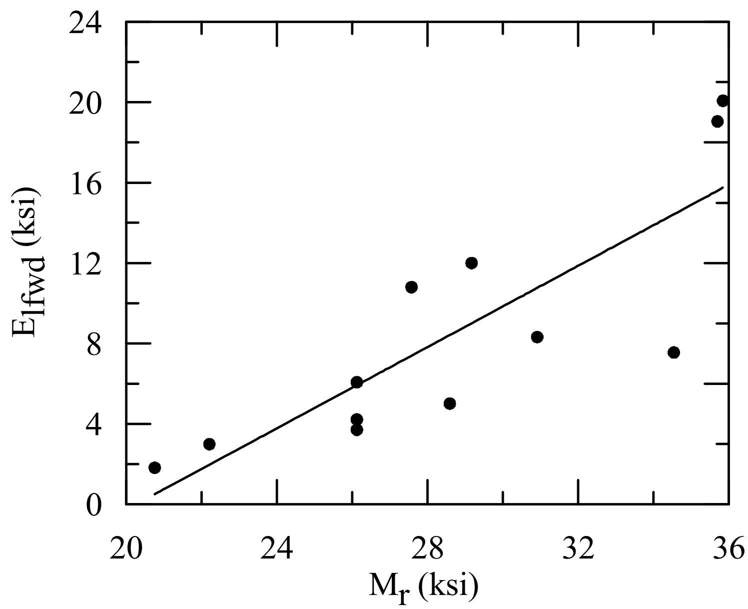

Figure 29
Variation of resilient modulus with E_{lfwd}

Table 39
A correlation matrix for the LFWD test results (r-value)

Variables	M_r	E_{lfwd}	P_{200}	P_4	γ_d	w
M_r	1	0.80	0.13	-0.67	0.41	0.62
E_{lfwd}	0.80	1	0.3	-0.65	0.48	0.49
P_{200}	0.13	0.3	1	-0.58	0.85	-0.13
P_4	-0.67	-0.65	-0.58	1	-0.52	-0.69
γ_d	0.41	0.48	0.85	-0.52	1	-0.10
w	0.62	0.49	-0.13	-0.69	-0.10	1

Table 40
Selections of the LFWD model parameters

Model parameters	RMSE (ksi)	R^2
$M_r, Elfwd^{0.21}$	2.77	0.70
$M_r, Elfwd^{0.11}, P_4$	2.35	0.77
$M_r, Elfwd^{0.21}, P_{200}$	2.89	0.70
$M_r, Log(Elfwd), \frac{\gamma_d}{w}$	5.82	0.23
$M_r, Log(Elfwd), P_4$	4.34	0.31
$M_r, Log(Elfwd)$	6.58	0.72

Table 41
Regression analysis for the LFWD – direct model

Model	Parameter estimated	Pr> F (p-value)	Pr> | t | (p-value)
$M_r, Elfwd^{0.21}$	Model	0.0001	-
	$Elfwd^{0.21}$	-	0.0001

Table 42
Regression analysis for the LFWD – material property model

Model	Parameter estimated	Pr> F (p-value)	Pr> | t | (p-value)
$M_r, Elfwd^{0.11}, P_4$	Model	< 0.0001	-
	$Elfwd^{0.11}$	-	< 0.0001
	p_4	-	0.008

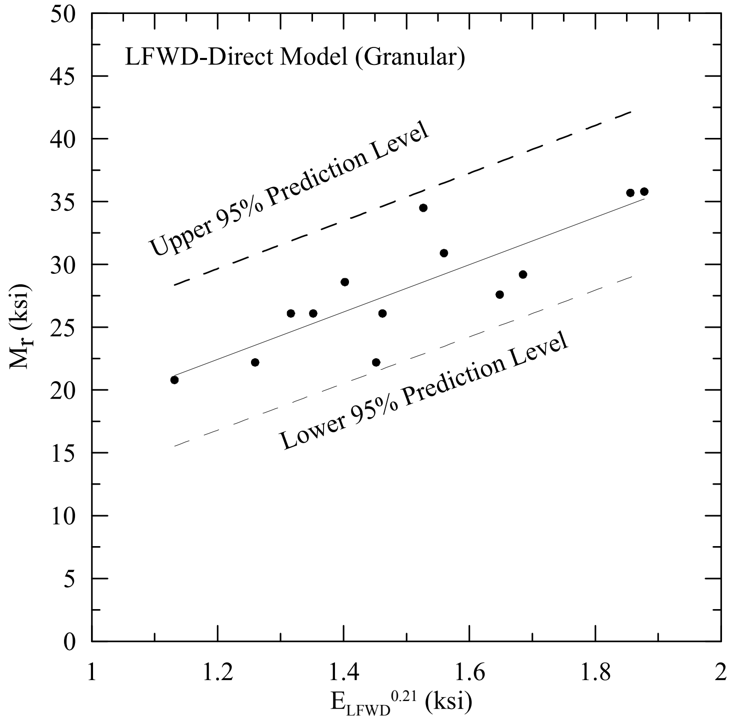

Figure 30
Predictions from the LFWD – direct model

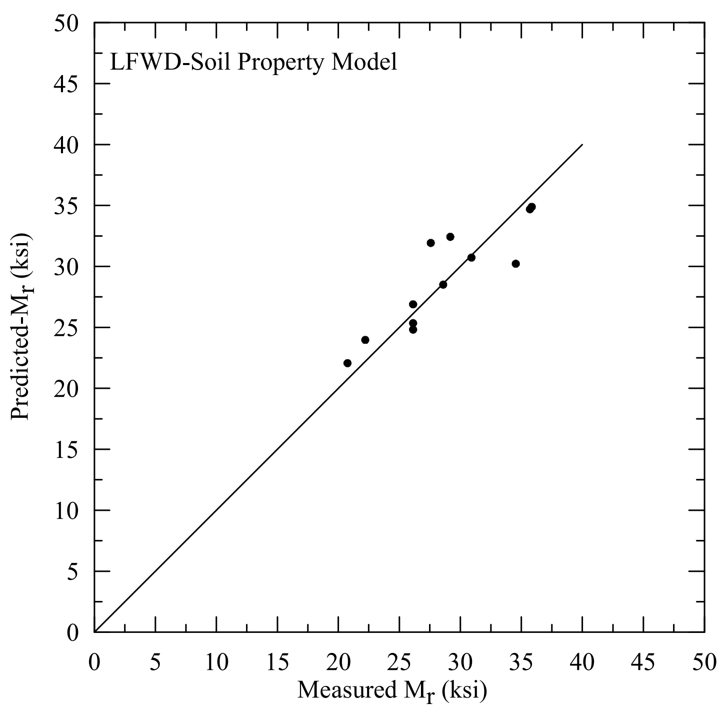

Figure 31
Predictions from the LFWD – soil property model

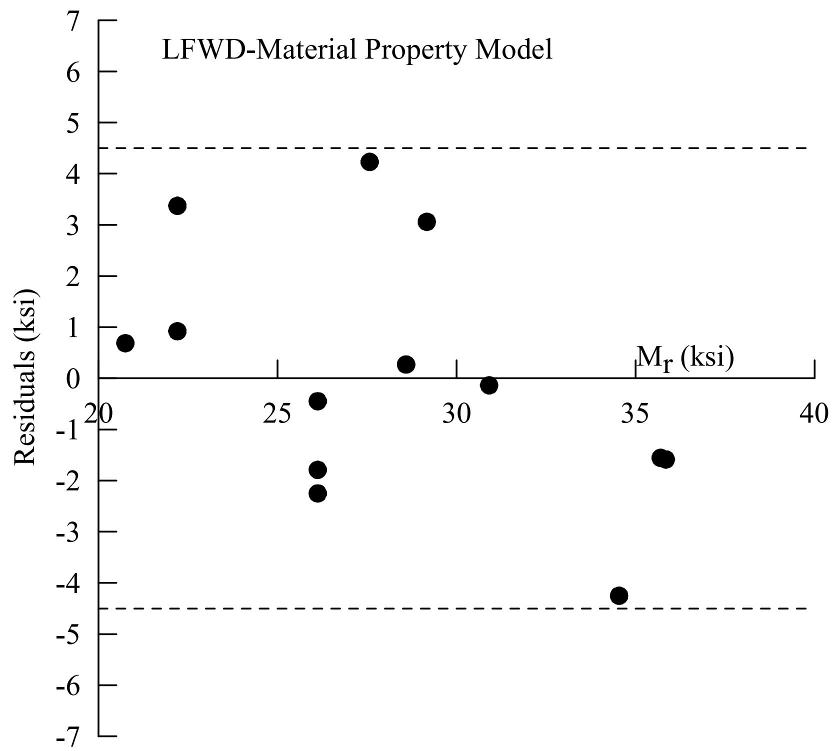

Figure 32
Residuals from LFWD – material property model

SUMMARY AND CONCLUSIONS

This report presents a summary of the development of regression models that predict the resilient modulus of cohesive and granular materials using the test results of DCP, LFWD, and GeoGauge and properties of tested material. Field and laboratory testing programs were conducted. The field testing program included DCP, LFWD, and GeoGauge testing, whereas the laboratory program included repeated load triaxial resilient modulus tests and physical properties and compaction tests. Comprehensive regression analyses were conducted on the laboratory and field test results. M_r prediction models were developed for cohesive and granular soils. Table 43 summarizes the models developed in this study. Based on the results of this study, the following conclusions can be drawn:

- Regression models were developed to predict the resilient modulus of cohesive soils and granular materials from the test results of DCP, GeoGauge, LFWD, and material physical properties.
- In general, good agreements were obtained between the resilient modulus values predicted from the proposed models and those measured in the repeated load triaxial resilient modulus test.
- The resilient modulus, DCP, GeoGauge, and LFWD test results were influenced by the moisture content, dry unit weight, and other physical properties of the tested soils.
- The DCP – soil property model had the best prediction of resilient modulus of cohesive soils, followed by the DCP – direct model and GeoGauge-direct model.
- The GeoGauge – material property model was the best in predicting the resilient modulus of granular materials, followed by the DCP-material property model.

Table 43
Summary of the resilient modulus prediction models

Method	Model	Coefficient of determination (R^2)	Mr Range (ksi)
M_r Prediction Models for Cohesive Soils – Direct			
DCP – Direct Model	$M_r = \frac{151.8}{(DCPI)^{1.096}}$	0.9	1-14
GeoGauge – Direct Model	$M_r = 6.74 + 0.03E_{geo}^{1.54}$	0.59	5.6-12.1
LFWD – Direct Model	$M_r = 5.70E_{lfwd}^{0.18}$	0.54	5.6-12.1
M_r Prediction Models for Cohesive Soils – Material Property			
DCP – Material Property Model	$M_r = 0.56 + 293.2\left(\frac{1}{DCPI^{1.46}}\right) + 89.9\left(\frac{1}{w^{1.27}}\right)$	0.92	1-14
GeoGauge – Material Property Model	$M_r = -2.023 + 0.027\left(E_{geo}^{0.8}\right) + 87.24\left(\frac{1}{w^{0.78}}\right)$	0.72	5.6-12.1
LFWD – Material Property Model	$M_r = 1.63 + 2.7\left(E_{lfwd}^{0.2}\right) + 35.17\left(\frac{1}{w}\right)$	0.70	5.6-12.1
M_r Prediction Models for Granular Soils – Direct			
DCP – Direct Model	$M_r = \frac{56.73}{DCPI^{0.23}}$	0.77	20.8-43.3
GeoGauge – Direct Model	$M_r = 36.68LOG(E_{geo}) - 7.21$	0.82	20.8-43.3
LFWD – Direct Model	$M_r = 18.69E_{lfwd}^{0.21}$	0.70	20.8-43.3
M_r Prediction Models for Granular Soils – Material Property			
DCP – Material Property Model	$M_r = \frac{53.74}{DCPI^{0.15}} - 0.07p_4$	0.82	20.8-43.3
GeoGauge – Material Property Model	$M_r = 35.38LOG(E_{geo}) - 0.06p_4 - 0.39p_{200}$	0.88	20.8-43.3
LFWD – Material Property Model	$M_r = 27.48Elfwd^{0.11} - 0.08P_4$	0.77	20.8-43.3

Legend: DCPI – Dynamic cone penetration index (mm/blow), E_{geo} – Modulus from GeoGauge (ksi), M_r – Resilient modulus (ksi), E_{lfwd} – LFWD modulus (ksi), γ_d – Dry unit weight (pcf), w – Water content (%), p200 – Percent passing 0.075 mm (No. 200) sieve, p4 – Percent passing 4.75 mm (No. 4) sieve

RECOMMENDATIONS

This report presents the results of a study conducted to develop resilient modulus prediction models of cohesive and granular soils from different in situ tests such as dynamic cone penetrometer, light falling weight deflectometer, and GeoGauge for possible application in construction control of pavement layers. The approach of predicting the M_r from the models developed in this study will help in the implementation of stiffness based QA/QC procedures during the construction of pavement layers. It is noted that these models are mainly applicable to the soils' types with physical properties presented in this report.

The following initiatives are recommended in order to facilitate the implementation of this study:

1. Implement the DCP device in the resilient modulus based QC/QA procedure during and after the construction of pavement layers and embankments.

2. Initiate a research project to implement and verify the M_r prediction models for cohesive soils. The research project should include different field projects covering various types of cohesive soils.

3. Validate the M_r prediction models for granular soils. The M_r prediction models that were developed in this study for granular soils were derived based on limited data points, and hence they can be used for a relatively narrow M_r range. Therefore, future studies should be performed to incorporate more granular soils with a wider M_r range, which will enhance the prediction of granular soils' M_r.

REFERENCES

1. Louisiana Standard Specifications for Roads and Bridges. Louisiana Department of Transportation and Development, Baton Rouge, Louisiana, 2000.

2. National Cooperative Highway Research Program (NCHRP). Guide for Mechanistic-Empirical Design of New and Rehabilitated Pavement Structures, Part2, Design Inputs, NCHRP 1-37A, Final Report, March 2004.

3. Nazzal, M.D., "Field Evaluation of In situ Test Technology for QC/QA During Construction of Pavement Layers and Embankments." Master Thesis, Louisiana State University, 2003.

4. Abu-Farsakh, M.Y; Alshibli, K.; Nazzal, M. D.; and Seyman, E. *Assessment of In Situ Test Technology for Construction Control of Base Courses and Embankments*. Final Report No. 385, Louisiana Transportation Research Center, Baton Rouge, Louisiana, 2004.

5. Mohammad, L.N.; Gaspard, K.; Herath, A.; and Nazzal, M. D. "Comparative Evaluation of Subgrade Resilient Modulus from Non-destructive, In situ, and Laboratory Methods." Final Report No. 417, Louisiana Transportation Research Center, 2007.

6. Mohammad, L.N.; Huang, B.; Puppala, A.; and Alen, A.A. "A Regression Model for Resilient Modulus of Subgrade Soils." *Transportation Research Record*, No. 1687, National Research Council, Washington, D.C., 1999, pp. 47–54.

7. Van Til, M.; McCullough, B.; Vallerga, B.; and Hicks, R.; *Evaluation of AASHTO Interim Guides for Design of Pavement Structures*, Report NCHRP 128, Highway Research Board, 1972.

8. Sawangsuriya, A.; Edil, T.B.; and Bosscher, P.J. "Comparison of Moduli Obtained from the Soil Stiffness Gauge with Moduli from Other Tests." *CD-ROM of the 81st Annual Meeting of the Transportation Research Board*, Washington, D.C., 2002.

9. Egorov, K.E. "Calculation of Bed for Foundation with Ring Footing." *Proc. 6th International Conference on Soil Mechanics and Foundations Engineering*, Vol. 2, 1965, pp. 41– 45.

10. Zorn Company. "Test Device and Road Construction." http://www.Zorn-online.de/er/products/td-rc, Germany, 2001.

11. Carl Bro Pavement Consultants. User Guide of the LFWD, Denmark, 2000.

12. Hassan, A. "The Effect of Material Parameters on Dynamic Cone Penetrometer Results for Fine-Grained Soils and Granular Base materials." Ph.D. Dissertation, Oklahama State University, Stillwater, 1996.

13. George, K.P. and Uddin, W. “Subgrade Characterization for Highway Pavement Design.” Department of Civil Engineering, University of Mississippi, Final Report, MS-DOT-RD-00-131, 2000.

14. Webster, S.L.; Brown, R.W.; and Porter, J.R. “Force Projection Site Evaluation Using the Electric Cone Penetrometer and the Dynamic Cone Penetrometer.” U.S. Waterways Experimental Station, Report GL-94-17, 1994.

15. 17. Powell, W.D.; Potler, J.F.; Mayhew, H.C.; and Nunn, M.E., 1084. The Structural Design of Bituminous Roads. TRRL, Report LR 1,132, 62 pp., 1990.

16. AASHTO T 294-94. "Resilient Modulus of Unbound Granular Base/Subbase/ base Materials and Subgrade Soils – SHRP Protocol P46.” *American Association of State Highway and Transportation Officials*, T 294-94, 1995, pp. 794–807.

17. National Cooperative Highway Research Program (NCHRP). Project 1-28 A “Harmonized Test Methods for Laboratory Determination of Resilient Modulus For Flexible Pavement Design.” May, 2003.